UNIVERSITY OF GOTHENBURG

Do viscous flows slip?

Solving the Stokes equation with Hodge boundary conditions

Master's thesis in the Mathematical Sciences Master Program

BJÖRN SJÖSVÄRD

DEPARTMENT OF MATHEMATICAL SCIENCES
UNIVERSITY OF GOTHENBURG
Gothenburg, Sweden 2023
www.gu.se

Master's thesis 2023

Do viscous flows slip?

Solving the Stokes equation with Hodge boundary conditions

BJÖRN SJÖSVÄRD

UNIVERSITY OF GOTHENBURG

Department of Mathematical Sciences
University of Gothenburg
Gothenburg, Sweden 2023

Do viscous flows slip?
Solving the Stokes equation with Hodge boundary conditions

Björn Sjösvärd

Supervisor: Andreas Rosén, Department of Mathematical Sciences
Examiner: Irina Pettersson, Department of Mathematical Sciences

Master's Thesis 2023
Department of Mathematical Sciences
University of Gothenburg

Abstract

In this thesis, the Stokes equation is discussed and solved under different boundary conditions. The Stokes equation governs the flow of viscous liquids, for example honey or syrup. The first chapters in the thesis provides an introduction to multivector algebra and analysis, with the aim of presenting the concept of Hodge decompositions. With an application of this theory, the Stokes equation with the Hodge boundary conditions is solved using the finite element method. This is compared to the solution of the Stokes equation under the more standard no-slip condition. It is concluded that the Hodge boundary conditions are natural from a mathematical point of view, although they can not be used to model physical flows. In particular, they are contrary to the known physical fact that viscous flows tend to stick to the boundary. Moreover, it is showed that the Hodge boundary conditions can be interpreted in a way that the friction at the boundary of the domain is solely determined by the curvature.

Keywords: Mathematics, partial differential equations, multivectors, Hodge decompositions, the Stokes equation, Hodge boundary conditions.

Acknowledgements

First of all I would like to thank my supervisor Andreas Rosén for proposing an interesting project and supporting my work throughout the process. The study of multivectors has been an eye-opener in many ways. I would also like to thank my former boss, principal Pär Holmertz at Nösnäsgymnasiet, who has been a great inspiration to how one can follow ones own path, Mattias Kauttmann for helping me building my confidence to start to do so, and my girlfriend Sofia Rydén for believing in me in times when the project has been difficult. Lastly I would also like to thank my congregation in Munkegärdekyrkan for helping me stay focused at what is really important in life and the two cats Brody and Åke for invaluable company during the project. Mathematics is truly beautiful.

Björn Sjösvärd, Ytterby, June 2023

Contents

CHAPTER 1

Introduction

The *Stokes equation* describes the flow of an incompressible, viscous liquid in a bounded region. It is derived from some simplifications of the Navier-Stokes equations and is formulated

$$\begin{cases} \nabla p - \mu \Delta v = f, \\ \operatorname{div}(v) = 0, \end{cases}$$

where the scalar function p is the pressure, the vector field v is the velocity, the constant μ is the viscosity constant, and f is the sum of the external forces acting on the liquid. A typical example of a liquid with high viscousity is honey. It is a known empirical fact that a viscous flow in a bounded region tends to stick to the boundary. For example, if one stirs honey in a jar, the honey close to the edges sticks to the jar. If D is the region bounded by the jar (the *domain*), this corresponds to the boundary condition $v|_{\partial D} = 0$, where ∂D is the boundary of the region (i.e., the jar itself). This is the standard boundary condition to use when solving the Stokes equation, and is in this thesis called the *no-slip boundary condition*. The main purpose of this project has been to solve the Stokes equation under another set of boundary conditions, and to investigate how these boundary conditions are to be interpreted. These boundary conditions are referred to as the *Hodge boundary conditions*, and besides constituting that the flow must be tangential at the boundary (i.e., it may not flow out of the bounded region) it also involves a condition on the vorticity. The Hodge boundary conditions do not, though, require the velocity to be zero at the boundary.

The first part of the project leading to this thesis consisted of a theoretical study of multivector fields and Hodge decompositions. Chapters 2 and 3 presents some of this theory. Apart from presenting the theory needed to fully understand the solution of the Stokes equation under the Hodge boundary conditions, these chapters also contain some interesting mathematical facts that show a glimpse of the utility of multivector analysis.

In Chapter 2, the concept of multivectors as well as some of their algebraic properties are introduced. In this chapter the reader also gets a presentation of how some basic concepts from multivector analysis can be used to put some well-known concepts from linear algebra and vector analysis in a more general framework. In particular, the differential operators in vector calculus (gradient, divergence, and curl) are generalised to multivector fields by the interior and exterior derivatives defined in Section 2.4, and the somewhat strange vector product, normally defined

only in three dimensions, is expressed as a composition of two different algebraic operations on multivectors.

In Chapter 3, the theory behind Hodge decompositions is presented. The exposition involves the solution of partial differential equations (PDE:s) with the finite element method (FEM), which is also briefly explained in Section 3.4. A Hodge decomposition, as it is mainly used in this thesis, is an orthogonal decomposition of a vector field $F \in L_2(D)$ into three components. One of these components belongs to a finite-dimensional subspace. The dimension of this particular subspace contains interesting information about the topology of the domain, and is the subject of Section 3.2. Among others, the Hodge decompositions can be used to show the unique solvability of boundary value problems. This is discussed in Section 3.3.

In Chapter 4, the Stokes equation is presented and solved for a two-dimensional domain under different boundary conditions. The first section, 4.1, serves as a brief introduction to the Stokes equation from a physical point of view. In Section 4.2, the Stokes equation is solved using the Hodge boundary conditions. The solution is a nice application of Hodge decompositions, leading to relatively easy computations where one in the end just needs to solve the Dirichlet and Neumann problems for the Poisson equation with homogeneus boundary conditions. It is also showed that the Hodge boundary conditions are to be interpreted in a way that they mean that the friction at the boundary is determined only by the geometry of the domain, which is one of the main results of the project. In Section 4.3, the Stokes equation is solved with the no-slip boundary condition, using the same external forces f as in the previous section. This is not possible using the Hodge decomposition in the same way as in Section 4.2, but is instead made in a more traditional way using a mixed finite element method.

To numerically compute Hodge decompositions and to numerically solve the Stokes equation, MATLAB has been used. The application pdeModeler has been used to construct triangulations of the domains, but other than that the code is written by the author (with a small exception; the first function in Appendix A.2) and is attached in full in the appendices of this thesis.

In summary, the two main points in this thesis is (1) that given the theory of Hodge decompositions, the Hodge boundary conditions are more natural than the no-slip boundary condition from a mathematical point of view even though they are not of physical relevance, and (2) that the Hodge boundary conditions are to be interpreted as that the friction at the boundary only depends on the curvature. These claims are supported by the presentation in Chapter 4, where one among other things can see that the solution of the Stokes equation under the no-slip boundary condition is rather mathematically involved and also has to face a few technical issues which are not present when using the Hodge boundary conditions. Apart from these main claims, there are also as mentioned above some points of mathematical interest made on the way. Some of the highlights can be found in Example 2.3.4 (the vector product), Example 2.4.3 (about the generalisations of gradient, divergence,

and curl), Theorem 3.1.6 (the main theorem on Hodge decompositions), and Section 3.2 (about the finitie-dimensional subspaces in the Hodge decompositions).

CHAPTER 2

Multivectors

In the first two chapters of the thesis, the theory needed to understand the solutions of the Stokes equation in Chapter 4 is presented. Some of the concepts have a standard main-stream notation, while others have not. In both cases, the notation in this thesis will in large follow Rosén [6]. This chapter presents the concept of multivectors and some of their algebraic properties. In Section 2.4 the exterior and interior derivatives are defined, and the section concludes by showing how these can be seen as generalisations of the different derivatives from vector calculus. The exterior and interior derivatives will play a major roll throughout the thesis.

2.1 k-vectors and multivectors

Throughout this thesis, V will be a vector space of dimension $1 \leq n < \infty$. In the main parts of this thesis, one may think of V as equal to $\mathbb{R}^2$ (or in some cases $\mathbb{R}^3$), although the theory in this and the next chapter applies more generally to affine spaces (see [6, chap. 2]). For any $0 \leq k \leq n$ one can construct a linear space $\wedge^k V$ of k-vectors, where a k-vector $w \in \wedge^k V$ can be interpreted as a k-dimensional object determined by its orientation and k-volume. In particular, when $k = 1$ and $V = \mathbb{R}^2$, one has $\wedge^1 V = V = \mathbb{R}^2$, and a 1-vector is simply a vector in the ordinary sense, with the $k-$volume defined by the ordinary vector length. 0-vectors will be referred to as *scalars*, 1-vectors as *vectors*, and 2-vectors as *bivectors*, and these are the most relevant k-vectors for this thesis since the computations where this theory is applied in Section 4.2 will be carried out in $\mathbb{R}^2$. In the presentation of the theory below, V will be an inner product space, which simplifies some of the notation and suffices for the purpose of this thesis. Recall that an inner product space V is a vector space over a field K with a map $\langle \cdot, \cdot \rangle : V \times V \to K$ called the inner product satisfying the following three properties:

$$\langle x, y \rangle = \overline{\langle y, x \rangle} \text{ (conjugate symmetry)},$$

$$\langle ax + by, z \rangle = a\langle x, z \rangle + b\langle y, z \rangle \text{ (linearity in first argument), and}$$

$$\langle x, x \rangle \geq 0 \text{ (positive definiteness)},$$

for all $x, y, z \in V$ and $a, b \in K$ with equality in the last property if and only if $x = 0$. In this thesis we will only consider real vector spaces, which means that the first property simplifies to $\langle x, y \rangle = \langle y, x \rangle$. For a more rigorous depiction of the theory of multivectors, which applies in a more general case, see Rosén [6, chap. 2].

If one knows a basis for the vector space V, one can determine a basis for the k-vector spaces $\wedge^k V$, using the definition below (2.1.1). The sign " $\wedge$ " appearing in the definition denotes the exterior product, which will be presented in some more detail in Section 2.2.

Definition 2.1.1. [6, pp. 27f]
Let V be a vector space of dimension n with basis $\{e_1, ..., e_n\}$. Let $s \subset \{1, 2, ..., n\}$ and $|s|$ be the number of elements in s. Then $\{e_s\}_{|s|=k}$ is called the *induced basis* for $\wedge^k V$ where $e_s := e_{s_1} \wedge ... \wedge e_{s_k}$ if $s = \{s_1, ..., s_k\}$ with $s_1 < ... < s_k$.

For example, if $V = \mathbb{R}^3$ is a vector space with basis $\{e_1, e_2, e_3\}$, then $\{e_1 \wedge e_2, e_1 \wedge e_3, e_2 \wedge e_3\}$ is the induced basis for the bivector space $\wedge^2 V$. We will often use a shorthand notation, where the indices for the basis element will be concatenated instead of writing out the wedge between them, such that for example $e_j \wedge e_k \wedge e_l := e_{jkl}$. The basis for the bivector space just mentioned can thus instead be written as $\{e_{12}, e_{13}, e_{23}\}$. The concept of *multivectors* below is defined in a general sense. For the most part in the following, though, we will restrict the attention to homogeneous multivectors in $\mathbb{R}^2$.

Definition 2.1.2. [6, p. 30]
Define the *exterior algebra* of V to be the direct sum

$$\wedge V := \wedge^0 V \oplus \wedge^1 V \oplus ... \oplus \wedge^n V.$$

An element $w = w_0 + w_1 + ... + w_n \in \wedge V$ is called a *multivector*. A multivector $w \in \wedge^k V$ for some k is called a *homogeneous* multivector of *degree k*.

Geometrically, the bivector $e_{12} \in \wedge^2 V$ can be thought of as a two-dimensional object, the parallelogram spanned by e_1 and e_2. For $V = \mathbb{R}^3$, a $3-$vector e_{123} can similarly be thought of as a three-dimensional object.

2.2 Exterior and interior products

The exterior and interior products are products on $\wedge V$, where the first one has a standard notation while the second one has not. The exterior product is associative, meaning that $(v_1 \wedge v_2) \wedge v_3 = v_1 \wedge (v_2 \wedge v_3)$ for all $v_1, v_2, v_3 \in \wedge V$, and has two well-known properties that are frequently used in calculations. The first one is that $v_1 \wedge ... \wedge v_k = 0$ if $v_i = v_j$ for some $i \neq j$. The second is that the product changes sign when two elements are interchanged. For example, $e_1 \wedge e_2 = -e_2 \wedge e_1$. Since the computations in this thesis will be carried out mainly in $\mathbb{R}^2$ (and in a few cases in $\mathbb{R}^3$), it is enough to know these two properties and how to multiply scalars or scalar

functions. Below is an example where the exterior product of two multivectors is calculated.

Example 2.2.1.
Let $v = 2e_1 - e_2 + e_{12}$ and $w = 3 + 5e_1$. Computing the exterior product $v \wedge w$, one gets

$$\begin{aligned} v \wedge w &= (2e_1 - e_2 + e_{12}) \wedge (3 + 5e_1) \\ &= 2 \cdot 3e_1 + 2 \cdot 5e_1 \wedge e_1 - 3e_2 - 5e_2 \wedge e_1 + 3e_{12} + 5e_{12} \wedge e_1 \\ &= 6e_1 + 10 \cdot 0 - 3e_2 - 5e_{21} + 3e_{12} + 5 \cdot 0 \\ &= 6e_1 - 3e_2 + 5e_{12} + 3e_{12} \\ &= 6e_1 - 3e_2 + 8e_{12}. \end{aligned}$$

As can be seen above, in practice, the computation of the exterior product is carried out by multiplying the scalars term by term and cocatenating the indices of the basis elements, and thereafter using the two above-mentioned properties to simplify the expression. For the purpose of this thesis, we do not have to be more formal than this when it comes to the exterior product. To conclude the part about the exterior product, we give a definition which can be useful in some cases when one should determine the sign of $e_s \wedge e_t$ where e_s and e_t are multivectors with $s, t \subset \bar{n} := \{1, 2, ..., n\}$. We will also use it in the proof of Proposition 2.3.3.

Definition 2.2.2. [6, p. 32]
For subsets $s, t \subset \bar{n} := \{1, 2, ..., n\}$, let

$$\epsilon(s, t) := (-1)^{|\{(s_i, t_j) \in s \times t : s_i > t_j\}|},$$

where $s \times t$ denotes the Cartesian product, be the sign of the permutation that rearranges $s \cup t$ in increasing order.

With the above definition,

$$e_s \wedge e_t = \begin{cases} \epsilon(s, t) e_{s \cup t}, \text{ if } s \cap t = \varnothing \\ 0, \text{ if } s \cap t \neq \varnothing. \end{cases}$$

The *interior product* (or the interior *products*, left- respectively right interior product) is, when V is restricted to be an inner product space, a bilinear product on $\wedge V$. Formally, it can be defined as the operation adjoint to exterior multiplication

[6, pp. 51f]. We start by describing how one computes with it. Let $\dim(V) = n$ with $\{e_i\}$ a basis for V and $\bar{n} = \{1, 2, ..., n\}$ where $s \subset \bar{n}$ is a subset and $j \in \bar{n}$. One can then compute the left ($\lrcorner$) interior product by using

$$e_j \lrcorner e_s = \begin{cases} (-1)^k e_{s\setminus\{j\}}, \text{ if } j \in s \\ 0, \text{ if } j \notin s, \end{cases}$$

where k is the number of elements in s strictly smaller than j. In words, one removes the index in the basis element on the left hand side from the basis element's indices on the right hand side and computes the sign by counting how many indices there are on the right hand side that are strictly smaller than the index on the left hand side. In the main computations of this thesis (for example in Section 4.2), this is an easy task since we have no more than two or maybe three indices. If the index from the left hand side does not appear on the right hand side, the result of the left interior product is always zero. The scalars (or scalar functions) are multiplied term by term, just as in the case for the exterior product. Computations with the right interior product are carried out in essentially the same way. The only difference between $e_j \lrcorner e_s$ and $e_s \llcorner e_j$ is possibly the sign. One can define

$$e_j \llcorner e_s = \begin{cases} (-1)^m e_{s\setminus\{j\}}, \text{ if } j \in s \\ 0, \text{ if } j \notin s, \end{cases}$$

where m is the number of elements in s strictly larger than j. Below is a simple example of a computation with the left interior product.

Example 2.2.3.
Let $v_1 = 3e_1 + 4e_2$ and $w_1 = 2e_1 - 3e_2 + e_{12}$. Then, the left interior product

$$\begin{aligned} v_1 \lrcorner w_1 &= (3e_1 + 4e_2) \lrcorner (2e_1 - 3e_2 + e_{12}) \\ &= 3 \cdot 2e_1 \lrcorner e_1 - 3 \cdot 3e_1 \lrcorner e_2 + 3e_1 \lrcorner e_{12} + 4 \cdot 2e_2 \lrcorner e_1 - 4 \cdot 3e_2 \lrcorner e_2 + 4e_2 \lrcorner e_{12} \\ &= 6 - 9 \cdot 0 + 3e_2 + 8 \cdot 0 - 12 + 4 \cdot (-1)^1 e_1 \\ &= 6 + 3e_2 - 12 - 4e_1 \\ &= -6 - 4e_1 + 3e_2. \end{aligned}$$

Moreover, as opposed to the exterior product, the interior products are not associative, that is, in general $(a \lrcorner b) \lrcorner c \neq a \lrcorner (b \lrcorner c)$, and likewise for the right interior product, but they satisfy the following important relations [6, p. 53]:

$$\text{a) } (v_1 \wedge v_2) \lrcorner w = v_2 \lrcorner (v_1 \lrcorner w),$$

$$\text{b) } (v_1 \lrcorner w) \llcorner v_2 = v_1 \lrcorner (w \llcorner v_2),$$

$$\text{c) } w \llcorner (v_1 \wedge v_2) = (w \llcorner v_2) \llcorner v_1,$$

and

$$\text{d) } v \lrcorner w = (-1)^{l(k-l)} w \llcorner v, w \in \wedge^k V, v \in \wedge^l V.$$

Below is an illustration of a typical way one of these relations will be used.

Example 2.2.4.
Let $v_2 = 2e_1 - e_2 + 2e_{12}$ and $w_2 = e_{12}$. Computing the left interior product $v_2 \lrcorner w_2$, we get

$$\begin{aligned} v_2 \lrcorner w_2 &= (2e_1 - e_2 + 2e_{12}) \lrcorner e_{12} \\ &= 2e_1 \lrcorner e_{12} - e_2 \lrcorner e_{12} + 2e_{12} \lrcorner e_{12} \\ &= (-1)^0 \cdot 2e_2 - (-1)^1 e_1 + 2e_2 \lrcorner (e_1 \lrcorner e_{12}) \\ &= 2e_2 + e_1 + 2 \cdot (-1)^0 e_2 \lrcorner e_2 \\ &= 2e_2 + e_1 + 2 \\ &= 2 + e_1 + 2e_2. \end{aligned}$$

Note the use of property a) between the second and the third row.

In the following parts of this thesis we will mostly use the left interior product, but in a few cases we will also use encounter the right interior product. Therefore, it can be worth noting that by relation d) above, $w_1 \llcorner v_1 = -v_1 \lrcorner w_1 = 6 + 4e_1 - 3e_2$, while $w_2 \llcorner v_2 = v_2 \lrcorner w_2$ in Example 2.2.4. It is thus important to keep track of the sign when dealing with the interior products, but relation d) gives a convenient way to swap from the right to the left interior product.

As a last remark of this section, for the case $e_s \lrcorner e_t$ with $|s|, |t| > 1$, instead of repeatedly use relation a) above, Definition 2.2.2 can be used to compute

$$e_s \lrcorner e_t = \begin{cases} \epsilon(s, t \setminus s) e_{t \setminus s}, \text{ if } s \subset t \\ 0, \text{ if } s \not\subset t \end{cases} \quad \text{and}$$

$$e_t \llcorner e_s = \begin{cases} \epsilon(t \setminus s, s) e_{t \setminus s}, \text{ if } s \subset t \\ 0, \text{ if } s \not\subset t. \end{cases}$$

Again, in the parts of this thesis where this theory is applied, we will very rarely have $|s| > 2$, so the rules described before Example 2.2.4 and the relations a)-d) above will suffice for our purposes. In a few cases we will also encounter the inner product of two multivectors. If we demand that the induced basis $\{e_s\}_{|s|=k}$ for $\wedge^k V$ (see Defintion 2.1.1) is an ON-basis whenever $\{e_1, ..., e_n\}$ is an ON-basis for V, then we get a natural definition of the inner product. For example, if $\{e_1, e_2, e_3\}$ is an ON-basis for $\mathbb{R}^3$, then $\langle e_{12}, e_{12} \rangle = 1$ but $\langle e_{12}, e_{13} \rangle = 0$. In practice, if $v, w \in \wedge V$ are two

multivectors where $\dim(V) = n$, we can compute $\langle v, w\rangle = v_0 \lrcorner w_0 + v_1 \lrcorner w_1 + ... + v_n \lrcorner w_n$, where $v = v_0 + ... + v_n, w = w_0 + ... + w_n$, and all v_i, w_i are homogeneous multivectors of degree i. As a last note of this section, we also mention that we now can see the claim from earlier in this section that the inner product is the adjoint of the exterior product. Indeed, let $f, g, h \in \wedge V$. We then have, by the use of relation a) in this section

$$\begin{aligned}\langle f \wedge g, h\rangle &= (f \wedge g)_0 \lrcorner h_0 + (f \wedge g)_1 \lrcorner h_1 + ... + (f \wedge g)_n \lrcorner h_n \\ &= (f_0 \wedge g_0) \lrcorner h_0 + ((f_0 \wedge g_1) \lrcorner h_1 + (f_1 \wedge g_0) \lrcorner h_1) + ... \\ &= g_0 \lrcorner (f_0 \lrcorner h_0) + (g_1 \lrcorner (f_0 \lrcorner h_1) + g_0 \lrcorner (f_1 \lrcorner h_2)) + ... \\ &= \langle g, f \lrcorner h\rangle. \end{aligned} \tag{2.1}$$

This equality will be used in Section 3.1.

2.3 Hodge stars

The *Hodge star maps* will later be useful for solving the Stokes equation in Section 4.2. Again, we restrict our attention to an inner product space V.

Definition 2.3.1. Hodge star maps [6, p. 54]
Let $\dim(V) = n$, $w \in \wedge V$, and $e_{\bar{n}} = e_1 \wedge e_2 \wedge ... \wedge e_n$. Then, the *Hodge star maps* are

$$w \mapsto *w := e_{\bar{n}} \llcorner w,$$

$$w \mapsto w* := w \lrcorner e_{\bar{n}}.$$

Below are two examples where the first Hodge star map, $w \mapsto *w$, is applied to a bivector field and a vector field respectively, which illustrates a technique used in Section 4.2.

Example 2.3.2.
a) Let $w_1 = fe_{12}$ and $\bar{n} = \{1, 2\}$. Applying the Hodge star map, we get

$$*w_1 = e_{12} \llcorner fe_{12} = fe_{12} \lrcorner e_{12} = fe_2 \lrcorner (e_1 \lrcorner e_{12}) = fe_2 \lrcorner e_2 = f,$$

where we have used relations d) and a) from Section 2.2. So applying the Hodge star to the bivector field $w_1 = fe_{12}$ gives a scalar field with the same expression f.

b) Let $w_2 = ge_1 + he_2$ and again $\bar{n} = \{1, 2\}$. Applying the Hodge star map to this vector field, one gets

$$*w_2 = e_{12} \llcorner (ge_1 + he_2) = e_{12} \llcorner ge_1 + e_{12} \llcorner he_2 = ge_1 \lrcorner e_{12} + he_2 \lrcorner e_{12} = -he_1 + ge_2.$$

So by applying the Hodge star map to the vector field w_2, we have got a vector field $*w_2$ orthogonal to w_2.

Since the Hodge star maps will be frequently used, we formulate a proposition about some of their properties.

Proposition 2.3.3. *[6, pp. 55f]*
The Hodge star maps $*w$ and $w*$ have the following properties for all $w_i \in \wedge V$.
*a) They are each other's inverses, i.e., $(*w_1)* = w_1$ and $*(w_1*) = w_1$.*
b) They swap exterior and interior products in the following sense.

$$*(w_1 \wedge w_2) = (*w_2) \llcorner w_1, \;\; (w_2 \llcorner w_1)* = w_1 \wedge (w_2*),$$

$$(w_1 \wedge w_2)* = w_2 \lrcorner (w_1*), \;\; * (w_2 \lrcorner w_1) = (*w_1) \wedge w_2.$$

Proof.

a) By linearity of the interior product, it suffices to show the case $w_1 = e_s$. We have

$$(*e_s)* = (e_{\bar{n}} \llcorner e_s)* = \epsilon(\bar{n} \setminus s, s) e_{\bar{n} \setminus s} \lrcorner e_{\bar{n}} = (\epsilon(\bar{n} \setminus s, s))^2 e_s = e_s,$$

$$*(e_s) = *(e_s \lrcorner e_{\bar{n}}) = \epsilon(s, \bar{n} \setminus s) e_{\bar{n}} \llcorner e_{\bar{n} \setminus s} = (\epsilon(s, \bar{n} \setminus s))^2 e_s = e_s.$$

b) By using the definition of Hodge star map and relation c) above, one gets

$$*(w_1 \wedge w_2) = e_{\bar{n}} \llcorner (w_1 \wedge w_2) = (e_{\bar{n}} \llcorner w_2) \llcorner w_1 = (*w_2) \llcorner w_1.$$

Likewise, using relation a),

$$(w_1 \wedge w_2)* = (w_1 \wedge w_2) \lrcorner e_{\bar{n}} = w_2 \lrcorner (w_1 \lrcorner e_{\bar{n}}) = w_2 \lrcorner (w_1*).$$

To show $(w_2 \llcorner w_1)* = w_1 \wedge (w_2*)$, we let $w_2 = *w$. The left hand side then equals

$$((*w) \llcorner w_1)* = (*(w_1 \wedge w))* = w_1 \wedge w,$$

where the first equalities in a) and b) of this proposition are used. The right hand side equals the left hand side since

$$w_1 \wedge (w_2*) = w_1 \wedge ((*w)*) = w_1 \wedge w.$$

Lastly, setting $w_1 = w*$ and using the third equality in b) of this proposition, one gets

$$*(w_2 \lrcorner (w*)) = *((w \wedge w_2)*) = w \wedge w_2,$$
$$(*w_1) \wedge w_2 = (*(w*)) \wedge w_2 = w \wedge w_2,$$

proving the last identity. □

As mentioned earlier, the Hodge star maps will later prove to be very useful in the solution of the Stokes equation in Section 4.2. But as an interesting remark, we conclude this section by showing an example of how some basic concepts from linear algebra can be put in a more general context with the help of multivectors, the exterior and interior products, and the Hodge star maps.

Example 2.3.4. [6, pp. 58f]
Let $v_1 = x_1e_1 + y_1e_2 + z_1e_3$ and $v_2 = x_2e_1 + y_2e_2 + z_2e_3$. Consider the left Hodge star map applied to the exterior product

$$\begin{aligned} *(v_1 \wedge v_2) &= e_{123} \llcorner ((x_1e_1 + y_1e_2 + z_1e_3) \wedge (x_2e_1 + y_2e_2 + z_2e_3)) \\ &= e_{123} \llcorner ((x_1y_2 - x_2y_1)e_{12} + (x_1z_2 - x_2z_1)e_{13} + (y_1z_2 - y_2z_1)e_{23}) \\ &= (y_1z_2 - y_2z_1)e_1 + (x_1z_2 - x_2z_1)e_2 + (x_1y_2 - x_2y_1)e_3. \end{aligned}$$

As seen above, for $v_1, v_2 \in \wedge^1 V$ with $dim(V) = 3$, this agrees with the vector product. Note that the vector product in this way is a composition of two operators, and that the anticommutativity of the vector product is linked to the anticommutativity of the exterior product. Similarily, for $v_1, v_2, v_3 \in \wedge^1 V$ it can be shown that

$$\langle v_1, v_2 \times v_3 \rangle = *(v_1 \wedge v_2 \wedge v_3), \text{ and}$$
$$v_1 \times (v_2 \times v_3) = -v_1 \lrcorner (v_2 \wedge v_3).$$

2.4 Exterior and interior derivatives

The interior and exterior derivatives, defined for multivector fields, are two fundamental concepts in multivector analysis. The definition of the interior derivative uses the interior product, while the exterior derivative uses the exterior product and we will in the end of this section see how they generalise the concepts of *gradient*, *divergence*, and *curl* from vector calculus. Throughout this thesis, we use the nabla symbol $\nabla := \sum_{i=1}^{n} e_i \partial_i$.

Definition 2.4.1. [6, p. 212]
Let $D \subset X$ be an open set, (X, D) have dimension n, and $F : D \to \wedge V$ be a multivector field differentiable at $x \in D$. Then its *interior derivative* is defined by

$$\delta F(x) := \nabla \lrcorner F(x) = \sum_{i=1}^{n} e_i \lrcorner \partial_i F(x).$$

Its *exterior derivative* is defined by

$$dF(x) := \nabla \wedge F(x) = \sum_{i=1}^{n} e_i \wedge \partial_i F(x).$$

Note that the for a $k-$vector field F, we have $\delta F \in \wedge^{k-1} V$ and $dF \in \wedge^{k+1} V$. For example, the interior derivative of a vector field is a scalar field, while the exterior derivative is a bivector field. In the following sections, the usual case is that the exterior or interior derivative is applied to a vector field $F = f_1 e_1 + f_2 e_2$ in a two dimensional domain. Below are two concrete examples of computations with these derivatives.

Example 2.4.2.
Let $F = (x^2 + xy)e_1 + (y^3 - x^3)e_2 \in \wedge^1 V$. Then

$$\begin{aligned} dF &= \partial_1(x^2 + xy)e_{11} + \partial_1(y^3 - x^3)e_{12} + \partial_2(x^2 + xy)e_{21} + \partial_2(y^3 - x^3)e_{22} \\ &= 0 - 3x^2 e_{12} - x e_{12} + 0 \\ &= -(3x^2 + x)e_{12} \in \wedge^2 V, \text{ and} \end{aligned}$$

$$\begin{aligned} \delta F &= \partial_1(x^2 + xy)e_1 \lrcorner e_1 + \partial_1(y^3 - x^3)e_1 \lrcorner e_2 + \partial_2(x^2 + xy)e_2 \lrcorner e_1 + \partial_2(y^3 - x^3)e_2 \lrcorner e_2 \\ &= (2x + y) + 0 + 0 + (3y^2) \\ &= 2x + y + 3y^2 \in \wedge^0 V. \end{aligned}$$

One important shared property of the operators d and δ (pronounced *'del'*), is that they are nilpotent. Indeed, let F be a C^2 regular multivector field. Then we have

$$\begin{aligned} d^2F &= \nabla \wedge (\nabla \wedge F) \\ &= \nabla \wedge \left(\sum_{i=1}^{n} e_i \wedge \partial_i F \right) \\ &= \sum_{j=1}^{n} e_j \wedge \partial_j \left(\sum_{i=1}^{n} e_i \wedge \partial_i F \right) \\ &= \sum_{i,j=1}^{n} e_j \wedge e_i \wedge \partial_j \partial_i F \\ &= 0, \end{aligned}$$

using $e_i \wedge e_i = 0, e_i \wedge e_j = -e_j \wedge e_i$, and $\partial_j \partial_i F = \partial_i \partial_j F$, $\forall i, j$. Similarly,

$$\begin{aligned} \delta^2F &= \nabla \lrcorner (\nabla \lrcorner F) \\ &= \nabla \lrcorner \left(\sum_{i=1}^{n} e_i \lrcorner \partial_i F \right) \\ &= \sum_{j=1}^{n} e_j \lrcorner \partial_j \left(\sum_{i=1}^{n} e_i \lrcorner \partial_i F \right) \\ &= \sum_{i,j=1}^{n} e_j \lrcorner (e_i \lrcorner \partial_j \partial_i F) \\ &= \sum_{i,j=1}^{n} (e_j \wedge e_i) \lrcorner \partial_j \partial_i F \\ &= 0, \end{aligned}$$

using also relation a) in Section 2.2. The nilpotence of d and δ allows us to identify $(d+\delta)^2$ with the Laplace operator $\Delta := \sum_{i=1}^{n} \frac{\partial^2}{\partial {x_i}^2}$. For example, if $F = f_1 e_1 + f_2 e_2$ is a vector field, one has

$$\begin{aligned} (d+\delta)^2 F &= (d^2 + d\delta + \delta d + \delta^2) F \\ &= (d\delta + \delta d)(f_1 e_1 + f_2 e_2) \\ &= d(\partial_1 f_1 + \partial_2 f_2) + \delta((\partial_1 f_2 - \partial_2 f_1) e_{12}) \\ &= (\partial_1^2 f_1 + \partial_1 \partial_2 f_2) e_1 + (\partial_2 \partial_1 f_1 + \partial_2^2 f_2) e_2 + (\partial_1^2 f_2 - \partial_1 \partial_2 f_1) e_2 \\ &\quad - (\partial_2 \partial_1 f_2 - \partial_2^2 f_1) e_1 \\ &= (\partial_1^2 f_1 + \partial_2^2 f_1) e_1 + (\partial_1^2 f_2 + \partial_2^2 f_2) e_2 \\ &= (\Delta f_1) e_1 + (\Delta f_2) e_2 := \Delta F, \end{aligned}$$

which will be used in the following sections. To conclude this section we address the question of how the exterior and interior derivatives generalise the concepts of *gradient*, *divergence*, and *curl* from classical vector calculus. Below is an example showing this for the case $X = \mathbb{R}^3$ and $D \subset \mathbb{R}^3$ an open set.

Example 2.4.3.
For vector fields we use the basis $\{e_1, e_2, e_3\}$, and for bivector fields $\{e_{23}, e_{31}, e_{12}\}$ since we have the correspondences $*e_{23} = e_1, *e_{31} = e_2,$ and $* e_{12} = e_3$. Now let $F_0 : D \to \wedge^0 V$ be a scalar function. Then its exterior derivative

$$dF_0 = \partial_1 F_0 e_1 + \partial_2 F_0 e_2 + \partial_3 F_0 e_3,$$

equals the gradient ∇F_0.

Now let $F_1 : D \to \wedge^1 V, F_1 = f e_1 + g e_2 + h e_3$, be a vector field, where $f, g,$ and h are scalar functions. In this case the exterior derivative

$$\begin{aligned} dF_1 &= \partial_1 g e_{12} + \partial_1 h e_{13} + \partial_2 g e_{21} + \partial_2 h e_{23} + \partial_3 f e_{31} + \partial_3 g e_{32} \\ &= (\partial_2 h - \partial_3 g) e_{23} + (\partial_3 f - \partial_1 h) e_{31} + (\partial_1 g - \partial_2 f) e_{12}, \end{aligned}$$

corresponds to the curl of F_1, since $\mathrm{curl}(F_1) = *(dF)$. Computing the interior derivative, one gets

$$\delta F_1 = \partial_1 f + \partial_2 g + \partial_3 h,$$

which equal the divergence of F_1. Continuing with the bivector field $F_2 = a e_{23} + b e_{31} + c e_{12},$ where $a, b,$ and c are scalar functions, one gets that the exterior derivative

$$dF_2 = (\partial_1 a + \partial_2 b + \partial_3 c) e_{123},$$

which one recognises as the divergence, or to be precise $\mathrm{div}(*F_2) = *(dF_2)$. Computing the interior derivative,

$$\begin{aligned} \delta F_2 &= -\partial_1 b e_3 + \partial_1 c e_2 + \partial_2 a e_3 - \partial_2 c e_1 - \partial_3 a e_2 + \partial_3 b e_1 \\ &= (\partial_3 b - \partial_2 c) e_1 + (\partial_1 c - \partial_3 a) e_2 + (\partial_2 a - \partial_1 b) e_3, \end{aligned}$$

one can see that this equals $-\mathrm{curl}(*F_2)$. Lastly, if $F_3 = F e_{123} \in \wedge^3 V$, for a scalar function F, the interior derivative equals

$$\delta F_3 = \partial_1 F e_{23} + \partial_2 F e_{31} + \partial_3 F e_{12},$$

corresponding to the gradient, since $\mathrm{grad}(*F_3) = *(\delta F_3)$.

This can be summarized in the following picture:

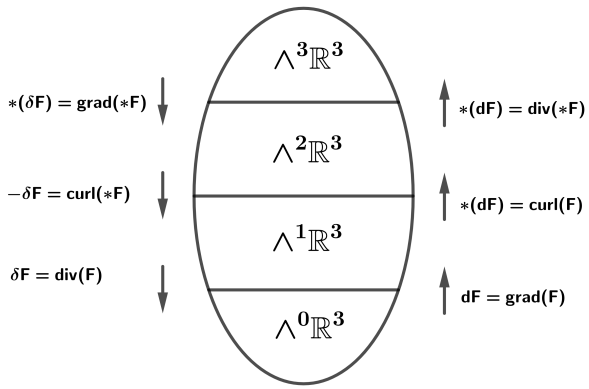

Figure 2.1: Relations between grad, div, and curl and concepts in multivector analysis, 3D.

For $V = \mathbb{R}^2$, we extend the definition $\nabla \times F$ of $\mathrm{curl}(F)$ for $F \in \wedge^1\mathbb{R}^3$ to $G \in \wedge^1\mathbb{R}^2$ by setting $\mathrm{curl}(G) = *(\nabla \wedge G)$, which is natural by Example 2.3.4. We then have the corresponding relations:

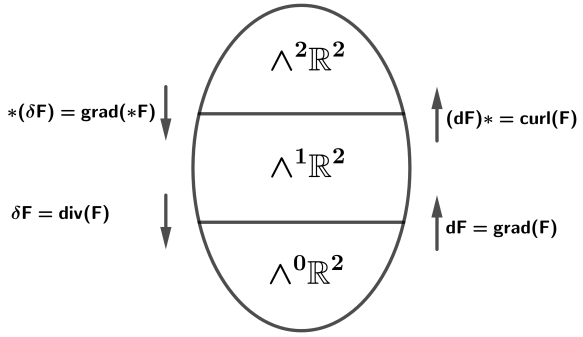

Figure 2.2: Relations between grad, div, and curl and concepts in multivector analysis, 2D.

CHAPTER 3

Hodge decompositions

In this chapter the goal is to present the concept of *Hodge decompositions*. A Hodge decomposition is an orthogonal splitting of the Hilbert space $L_2(D;\wedge V) := \{F : (\int_D |F(x)|^2 \,\mathrm{d}x)^{\frac{1}{2}} < \infty\}$ of square integrable multivector fields, where D is a bounded Lipschitz domain. A Lipschitz domain is a domain in Euclidean space where there is a requirement on the regularity of the boundary. In particular, any polygonal region or domain with a C^1-boundary is a Lipshitz domain. Theorem 3.1.6 implies the possibility to split any vector field $F \in L_2(D;\wedge V)$, where D is a bounded Lipschitz domain in Euclidean space, into three parts, $F = F_1 + F_2 + F_3$, where one of the parts belongs to a finite-dimensional subspace of $L_2(D;\wedge V)$. The two other parts belong to a subspace of curl free and a subspace of divergence free vector fields respectively. The subspaces in the decomposition are defined by using the exterior and interior derivatives from Section 2.4. In the following, we will use the notation $L_2(D) := L_2(D;\wedge V)$. Sometimes, when it is relevant, we will specify what type of $k-$vector field we are interested in by writing $L_2(D;\wedge^k)$. For example, if F is a vector field in the ordinary sense, we can write $F \in L_2(D;\wedge^1)$.

Definition 3.0.1. [6, p. 244]
Let D be a bounded Lipshitz domain in a Euclidean space with boundary ∂D and outward pointing unit normal $\hat{n}$. Define the following linear subspaces of $L_2(D)$, called *Hodge subspaces*:

$R(d) := \{F \in L_2(D) : F = \nabla \wedge U \text{ for some } U \in L_2(D)\}$,
$N(d) := \{F \in L_2(D) : \nabla \wedge F = 0\}$,
$R(\underline{\delta}) := \{F \in L_2(D) : F = \nabla \lrcorner U \text{ for some } U \in L_2(D) \text{ with } \hat{n} \lrcorner U = 0 \text{ on } \partial D\}$,
$N(\underline{\delta}) := \{F \in L_2(D) : \nabla \lrcorner F = 0 \text{ and } \hat{n} \lrcorner F = 0 \text{ on } \partial D\}$,
$C_{||}(D) := N(d) \cap N(\underline{\delta})$,
$R(\underline{d}) := \{F \in L_2(D) : F = \nabla \wedge U \text{ for some } U \in L_2(D) \text{ with } \hat{n} \wedge U = 0 \text{ on } \partial D\}$,
$N(\underline{d}) = \{F \in L_2(D) : \nabla \wedge F = 0 \text{ and } \hat{n} \wedge F = 0 \text{ on } \partial D\}$,
$R(\delta) := \{F \in L_2(D) : F = \nabla \lrcorner U \text{ for some } U \in L_2(D)\}$,
$N(\delta) := \{F \in L_2(D) : \nabla \lrcorner F = 0\}$,
$C_{\perp}(D) := N(\underline{d}) \cap N(\delta)$.

As for the L_2-space, we may sometimes write for example $R(d;\wedge^k)$ if we want to

specify what kind of k-vector field we are interested in. The lines under the operators in for example $R(\underline{d})$ correspond to a boundary condition. The additional demand $\hat{n} \wedge U = 0$ on ∂D means that $F \in R(\underline{d})$ is normal at the boundary, which is the case for all the fields belonging to one of the Hodge spaces above with the underlined $\underline{d}$. Similarly, for the spaces with $\underline{\delta}$, the fields are tangential at the boundary. This will be further discussed in Section 3.1. It is also important to note the inclusions $R(\underline{d}) \subset R(d) \subset N(d)$ and $R(\underline{\delta}) \subset R(\delta) \subset N(\delta)$. The last inclusions in these chains can be seen by the fact that d and δ are nilpotent operators (see Section 2.4). In this and the following chapter, just as in the definition above, $\hat{n}$ will always denote the outward pointing unit normal vector to the domain D. For an n-dimensional domain D, we will often use the notation $\hat{n} = \hat{n}_1 e_1 + ... + \hat{n}_n e_n$. To get an idea of what we are aiming at, the pictures below show an example of a Hodge decomposition of a vector field F[1].

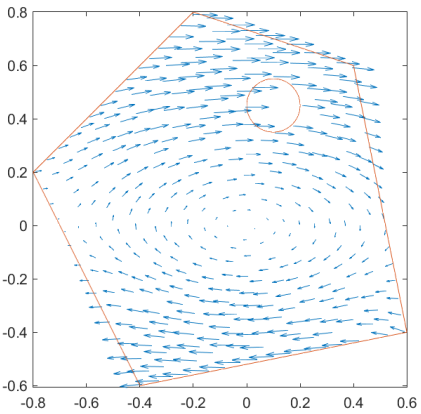

(a) A vector field F to be decomposed.

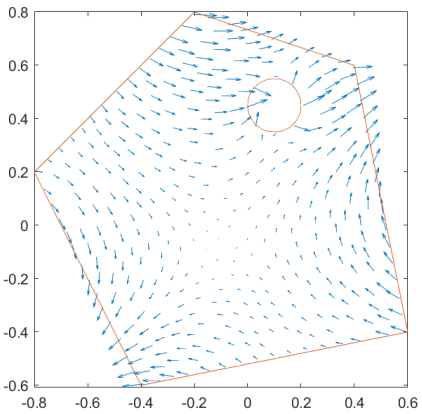

(b) The curl-free part, $F_1 \in R(d)$.

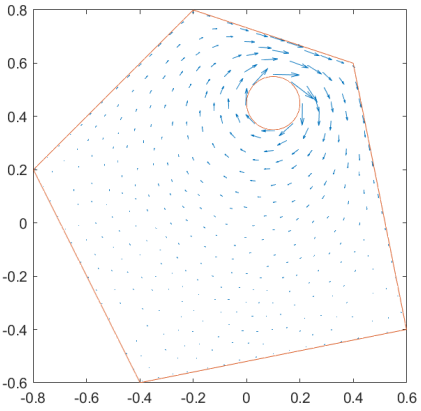

(c) $F_2 \in C_{||}(D)$.

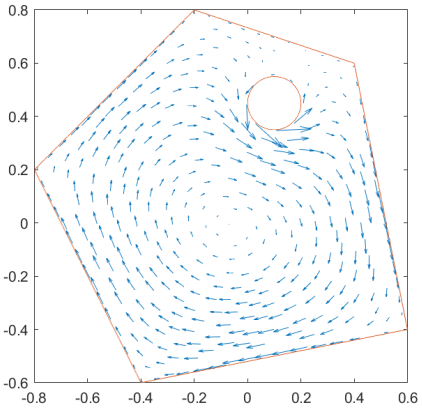

(d) The divergence-free part, $F_3 \in R(\underline{\delta})$.

Figure 3.1: Example of a Hodge decomposition, $F = F_1 + F_2 + F_3$. The curl-free part, F_1, is a gradient field. F_2 and F_3 are both tangential to the boundary. We shall later see (Section 3.2) that for a two-dimensional simply connected domain, i.e., a domain without a hole, we always have $F_2 = 0$ in a Hodge decomposition of a vector field $F \in L_2(D; \wedge^1)$.

[1] $F = (2y(1 - x^2 - y^2) + y - 3x^2y^3)e_1 - (2x(1 - x^2 - y^2) - x + 3x^3y)e_2$

3.1 Tangential and normal Hodge decompositions

The Hodge decompositions will play a major roll in the solution of the Stokes equation in Section 4.2, where we will have a simply connected domain $D \subset \mathbb{R}^2$. Before presenting the main theorem, we introduce some tools needed to understand the theory behind Hodge decompositions and to follow some of the proofs given in this section. The first proposition is presented for the sole purpose that it is used in the proof of Theorem 3.1.2.

Proposition 3.1.1. ***The parallelogram law*** *[2, p. 173]*
Let H be a Hilbert space. Then, for all $x, y \in H$,

$$\|x+y\|^2 + \|x-y\|^2 = 2(\|x\|^2 + \|y\|^2).$$

Proof.

$\|x+y\|^2 + \|x-y\|^2 = \|x\|^2 + 2Re\langle x, y\rangle + \|y\|^2 + \|x\|^2 - 2Re\langle x, y\rangle + \|y\|^2$
$= 2(\|x\|^2 + \|y\|^2)$. □

Theorem 3.1.2. *[2, pp. 173f]*
If V is a closed subspace of a Hilbert space H, then $H = V \oplus V^{\perp}$, where $V^{\perp}$ is the orthogonal complement of V.

Proof.

Given $x \in H$, let $\epsilon = \inf\{\|x-y\| : y \in V\}$ and $\{y_n\}$ be a sequence in V such that $\|x - y_n\| \to \delta, n \to \infty$. Using Proposition 3.1.1, one can write

$$2(\|y_n - x\|^2 + \|y_m - x\|^2) = \|y_n - y_m\|^2 + \|y_n + y_m - 2x\|^2.$$

Rewriting

$$\|y_n + y_m - 2x\|^2 = 4\|\frac{1}{2}(y_n + y_m) - x\|^2,$$

observing that $\frac{1}{2}(y_n + y_m) \in V$, and using the definition of ϵ one gets

$$\|y_n - y_m\|^2 = 2\|y_n - x\|^2 + 2\|y_m - x\|^2 - 4\|\frac{1}{2}(y_n + y_m) - x\|^2$$
$$\leq 2\|y_n - x\|^2 + 2\|y_m - x\|^2 - 4\epsilon^2.$$

As $m, n \to \infty$,

$$2\|y_n - x\|^2 + 2\|y_m - x\|^2 - 4\epsilon^2 \to 2\epsilon + 2\epsilon - 4\epsilon = 0,$$

so $\{y_n\}$ is a Cauchy sequence.

Now, let $y := \lim_{n\to\infty} y_n$ and $z := x - y$. Then, since V is closed, one has $y \in V$ and $\|x - y\| = \epsilon$. Next, we claim that $z \in V^\perp$. To see this, let $u \in V$ and define a function f by

$$f(t) := \|z + tu\|^2 = \|z\|^2 + 2t\langle z, u\rangle + t^2\|u\|^2.$$

The function f is real valued for $t \in \mathbb{R}$, and it attains its minimum value ϵ^2 at $t = 0$ because $z + tu = x - (y - tu)$ with $y - tu \in V$, and $f(0) = \|z\|^2 = \|x - y\|^2 = \epsilon^2$. Moreover,

$$f'(t) = 2\langle z, u\rangle + 2t\|u\|^2.$$

Thus, since $t = 0$ is a minimum, $f'(0) = 2\langle z, u\rangle{=}0$, which means that $\langle z, u\rangle = 0$ and $z \in V^\perp$, proving the claim.

By the claim above, one has $x = y + z$ with $y \in V$ and $z \in V^\perp$. It remains to show that the decomposition is unique. Assume that $x = y' + z'$ is another decomposition with $y' \in V$ and $z' \in V^\perp$. Then

$$y - y' = (x - z) - (x - z') = z' - z,$$

and since $y, y' \in V$ and $z, z' \in V^\perp$ one has

$$y - y' = z' - z \in V \cap V^\perp.$$

This means that $y - y'$ and $z' - z$ are orthogonal to themselves and hence are equal to zero. Thus we must have $y = y'$ and $z = z'$, which shows the uniqueness and completes the proof. □

Before stating the Hodge decomposition theorems, one more important fact is needed.

Theorem 3.1.3. *[6, pp. 354ff]*
Let D be a bounded Lipschitz domain in a Euclidean space. Then, $R(d), R(\delta), R(\underline{d})$, and $R(\underline{\delta})$ are closed subspaces of $L_2(D)$.

This theorem will not be proved in full, but we will make some important observations supporting the claim. Firstly, d and $-\underline{\delta}$ are formally adjoint operators, and so are δ and $-\underline{d}$. Indeed, let $D \subset \mathbb{R}^2$ be a bounded Lipschitz domain, $f \in L_2(D; \wedge^0)$ a scalar function, and $g \in L_2(D; \wedge^1)$ a vector field. Moreover, define a vector field $V(x) := \langle e_1 \wedge f(x), g(x)\rangle e_1 + \langle e_2 \wedge f(x), g(x)\rangle e_2$. By the divergence theorem, we have

$$\int_{\partial D} \hat{n}(y) \cdot V(y)\,\mathrm{d}y = \iint_D \mathrm{div}(V(x))\,\mathrm{d}x.$$

The left hand side of this equation equals

$$\int_{\partial D} \langle \hat{n}(y) \wedge f(y), g(y)\rangle\,\mathrm{d}y,$$

since

$$\begin{aligned}\hat{n}(y)\cdot V(y) &= \hat{n}_1(y)\langle e_1\wedge f(y), g(y)\rangle + \hat{n}_2(y)\langle e_2\wedge f(y), g(y)\rangle\\ &= \langle(\hat{n}_1(y)e_1+\hat{n}_2(y)e_2)\wedge f(y), g(y)\rangle\\ &= \langle \hat{n}(y)\wedge f(y), g(y)\rangle.\end{aligned}$$

By the observations in Example 2.4.3, Figure 2.2, $\operatorname{div}(V(x)) = \delta v(x)$. Thus, the right hand side equals

$$\begin{aligned}\iint_D \operatorname{div}(V(x))\,\mathrm{d}x &= \iint_D \partial_1\langle e_1\wedge f(x), g(x)\rangle + \partial_2\langle e_2\wedge f(x), g(x)\rangle\,\mathrm{d}x\\ &= \iint_D \langle e_1\wedge\partial_1 f(x), g(x)\rangle + \langle e_1\wedge f(x), \partial_1 g(x)\rangle + \langle e_2\wedge\partial_2 f(x), g(x)\rangle\\ &\quad + \langle e_2\wedge f(x), \partial_2 g(x)\rangle\,\mathrm{d}x\\ &= \iint_D \langle\nabla\wedge f(x), g(x)\rangle + \langle f(x), e_1\lrcorner\,\partial_1 g(x)\rangle + \langle f(x), e_2\lrcorner\,\partial_2 g(x)\rangle\,\mathrm{d}x\\ &= \iint_D \langle\nabla\wedge f(x), g(x)\rangle + \langle f(x), \nabla\lrcorner\, g(x)\rangle\,\mathrm{d}x.\end{aligned}$$

In this way, we have arrived at an equality we will use in several cases below, namely

$$\int_{\partial D}\langle\hat{n}(y)\wedge f(y), g(y)\rangle\,\mathrm{d}y = \iint_D \langle\nabla\wedge f(x), g(x)\rangle + \langle f(x), \nabla\lrcorner\, g(x)\rangle\,\mathrm{d}x. \tag{3.1}$$

Rewriting this and leaving out the variables and one of the integral signs on the right hand side for ease of notation, one can equivalently write

$$\int_D \langle f, \nabla\lrcorner\, g\rangle\,\mathrm{d}x = \int_{\partial D}\langle\hat{n}\wedge f, g\rangle\,\mathrm{d}y - \int_D\langle\nabla\wedge f, g\rangle\,\mathrm{d}x.$$

This means that for any f such that $\hat{n}\wedge f = 0$ on the boundary, $-d$ is the formally adjoint operator to δ. Since this requirement is precisely the boundary condition in $R(\underline{d})$, we conclude that the formally adjoint operator of δ is $-\underline{d}$. To show that d and $-\underline{\delta}$ are formally adjoint, one can be use the adjointness between the exterior and the interior product (see 2.1), from which one can conclude $\langle\hat{n}\wedge f, g\rangle = \langle f, \hat{n}\lrcorner\, g\rangle$. It can moreover be shown that δ and $-\underline{d}$ respectively d and $-\underline{\delta}$ are adjoint in the sense of unbounded operators[2], so by the Closed range theorem from functional analysis, $R(d)$ is closed if and only if $R(\underline{\delta})$ is closed and $R(\delta)$ is closed if and only if $R(\underline{d})$ is closed. It still remains, though, to argue for the closedness of one of the spaces in each pair. To narrow it down even further, one can show that $R(d)$ is closed if and only if $R(\delta)$ is closed. To see this, we apply the interior derivative to the (multi-) vector field $*F$, giving

$$\delta(*F) = \nabla\lrcorner\,(*F) = (\nabla*)\llcorner\, F = \pm F\lrcorner\,(\nabla*) = \pm(\nabla\wedge F)* = \pm(dF)*,$$

[2]This is beyond the scope of this thesis, but a proof can be found in [6, p. 353], Proposition 10.2.3.

where we have used the properties b) and d) from Section 2.2 and Proposition 2.3.3. We are thus left with the task to argue for the closedness of $R(d)$ *or* $R(\delta)$. To illustrate the main idea behind the proof, we turn our attention to $R(d)$. To prove that $R(d)$ is closed, one needs to show that any converging sequence $\{f_n\}$ converges to some $f \in R(d)$. If we let $u \in L_2(D; \wedge^0)$ and $f = du \in L_2(D; \wedge^1)$, this can be done by defining a linear, bounded operator $T : R(d; \wedge^1) \to L_2(D; \wedge^0)$ such that $Tf = u$. If this is possible, then $u_n = Tf_n$ converges to $u = Tf$, meaning that $du = f$ and thus $f \in R(d)$. One way to define the potential operator T is to use Poincaré's theorem (see [6, p. 240]). For our case, we start by letting

$$T'f = x \lrcorner \int_0^1 f(tx)\,\mathrm{d}t,$$

where $x \in D$. T' can also be expressed as a curve integral with notation from vector calculus. If $f = f_1 e_1 + ... + f_n e_n$ and $\gamma(t) = (tx_1, ..., tx_n)$, where $t \in [0, 1]$, is the straight line segment from the origin to a point $x = (x_1, ..., x_n)$, then

$$T'f = \int_0^1 f_1(xt)x_1 + ... + f_n(xt)x_n\,\mathrm{d}t.$$

The example below supports the claim that T' is a potential operator for $f \in R(d; \wedge^1)$.

Example 3.1.4.
Let $u = x^2y + xy$. We may then compute $f = du = (2xy + y)e_1 + (x^2 + x)e_2$. Applying T', we get

$$\begin{aligned} T'f &= (xe_1 + ye_2) \lrcorner \int_0^1 (2xyt^2 + yt)e_1 + (x^2t^2 + xt)e_2\,\mathrm{d}t \\ &= (xe_1 + ye_2) \lrcorner \left(\left(\frac{2xy}{3} + \frac{y}{2}\right)e_1 + \left(\frac{x^2}{3} + \frac{x}{2}\right)e_2\right) \\ &= x^2y + xy \\ &= u. \end{aligned}$$

Even though T' is a potential operator we have not shown that it is bounded (in the L_2-norm). Unfortunately, it is not, but there is a way to modify T' to become a bounded operator. The crucial fact needed to do so is that D is a bounded domain; it is for example not possible to do for the whole $\mathbb{R}^2$. The details can be found in [6, pp. 362ff], but the main idea is to modify the operator T' to an operator T by averaging over different base points for the curve integral.

Before stating the Hodge decomposition theorem, we formulate a Lemma which is proven with a similar application of the divergence theorem as we used to derive 3.1. It also gives an explanation to why there appear boundary conditions on some

of the subspaces appearing in Theorem 3.1.6 and Corollary 3.1.7.

Lemma 3.1.5.
$R(d)^\perp = N(\underline{\delta})$ and $R(\delta)^\perp = N(\underline{d})$.

Proof.

Let $u \in \wedge^k V$ and $g \in \wedge^{k+1} V$. If $g \in R(d)^\perp$, then we have $\int_D \langle \nabla \wedge u, g\rangle \, \mathrm{d}x = 0$. Moreover, by the divergence theorem,

$$\int_D \langle \nabla \wedge u, g\rangle \, \mathrm{d}x = \int_{\partial D} \langle \hat{n} \wedge u, g\rangle \, \mathrm{d}y - \int_D \langle u, \nabla \lrcorner g\rangle \, \mathrm{d}x,$$

for all u. In particular, we may choose a (non-constant) u that is equal to zero on the boundary. Then we see that a necessary condition for $g \in R(d)^\perp$ is that $\nabla \lrcorner g = 0$. And for any g such that $\nabla \lrcorner g = 0$, in order to have $g \in R(d)^\perp$ when $u|_{\partial D} \neq 0$, one sees that one also must have $\hat{n} \lrcorner g = 0$ on the boundary, since

$$\int_{\partial D} \langle \hat{n} \wedge u, g\rangle \, \mathrm{d}y = \int_{\partial D} \langle u, \hat{n} \lrcorner g\rangle \, \mathrm{d}y.$$

Thus, $R(d)^\perp = N(\underline{\delta})$. $R(\delta)^\perp = N(\underline{d})$ is shown in a similar way. Let now instead $u \in \wedge^{k+1} V$ and $g \in \wedge^k V$. The divergence theorem gives

$$\int_D \langle \nabla \lrcorner u, g\rangle \, \mathrm{d}x = \int_{\partial D} \langle \hat{n} \lrcorner u, g\rangle \, \mathrm{d}y - \int_D \langle u, \nabla \wedge g\rangle \, \mathrm{d}x,$$

from which one conclude that $g \in R(\delta)^\perp$ if and only if $\nabla \wedge u = 0$ and $\hat{n} \wedge g = 0$ on the boundary, since $\langle \hat{n} \lrcorner u, g\rangle = \langle u, \hat{n} \wedge g\rangle$. □

We are now ready to state the Hodge decomposition theorem, which will be crucial in Section 4.2.

Theorem 3.1.6. ***Tangential Hodge decomposition*** *[6, p. 245]*
Let D be a bounded Lipschitz domain in a Euclidean space. Then one has an orthogonal splitting

$$L_2(D) = R(d) \oplus C_{||}(D) \oplus R(\underline{\delta}),$$

where $R(d) \oplus C_{||}(D) = N(d), C_{||}(D) \oplus R(\underline{\delta}) = N(\underline{\delta})$, $C_{||}(D) := N(d) \cap N(\underline{\delta})$, and the tangential cohomology space $C_{||}(D)$ is finite-dimensional. At the level of $k-$vector fields, each $L_2(D; \wedge^k V)$ splits in this way.

Proof.

Theorem 3.1.3, Theorem 3.1.2 and Lemma 3.1.5 together give that $L_2(D) = R(d) \oplus N(\underline{\delta})$. Using the divergence theorem as in the proof of 3.1.5, with $F \in \wedge^k V$ and $G \in \wedge^{k+1} V$, one gets

$$\int_D \langle \nabla \wedge F, G \rangle \, \mathrm{d}x = \int_{\partial D} \langle F, \hat{n} \lrcorner G \rangle \, \mathrm{d}y - \int_D \langle F, \nabla \lrcorner G \rangle \, \mathrm{d}x.$$

If G is a field tangential at the boundary, and thus in particular $\hat{n} \lrcorner G = 0$ on ∂D, then one has

$$\int_D \langle \nabla \wedge F, G \rangle \, \mathrm{d}x = - \int_D \langle F, \nabla \lrcorner G \rangle \, \mathrm{d}x.$$

The left hand side vanishes for all tangential G exactly when $\nabla \wedge F = 0$, that is $F \in N(d)$, and the right hand side vanishes when F is orthogonal to $R(\underline{\delta})$. This shows that we also have a splitting $L_2(D) = R(\underline{\delta}) \oplus N(d)$. By the observations in the begging of this chapter, we have $R(d) \subset N(d)$. We claim also that $R(\underline{\delta}) \subset N(\underline{\delta})$. To see this, let $F = \nabla \lrcorner U \in R(\underline{\delta})$. By nilpotence, $\nabla \lrcorner F = 0$ is clear. Moreover,

$$\hat{n} \lrcorner F = \hat{n} \lrcorner (\nabla \lrcorner U) = \pm \hat{n} \lrcorner (U \llcorner \nabla) = \pm (\hat{n} \lrcorner U) \llcorner \nabla = 0,$$

where we have used Properties d) and b) from Section 2.2. Taking intersections of the two splittings $L_2(D) = R(d) \oplus N(\underline{\delta}) = R(\underline{\delta}) \oplus N(d)$ gives the desired splitting

$$L_2(D) = R(d) \oplus C_{||}(D) \oplus R(\underline{\delta}).$$

The finite-dimension of $C_{||}(D)$ will not be proven here, but discussed in Section 3.2. □

The name *tangential* Hodge decomposition is motivated by the fact that the fields in the space $R(\underline{\delta})$ and $C_{||}(D)$ are tangential to the boundary, as mentioned after Definition 3.0.1. To show that the boundary condition imposed on $R(\underline{\delta})$ means that the fields are tangential, we look at the case $R(\underline{\delta}; \wedge^1)$ in a two dimensional domain. Let $F = f_1 e_1 + f_2 e_2 = \nabla \lrcorner U \in L_2(D; \wedge^1)$ and φ be a scalar function with $\psi = \nabla \wedge \varphi$. By the divergence theorem, reasoning again as in the derivation of 3.1, and nilpotence of d, we may write

$$\begin{aligned} \int_D \langle \nabla \lrcorner U, \psi \rangle \, \mathrm{d}x &= \int_{\partial D} \langle \hat{n} \lrcorner U, \psi \rangle \, \mathrm{d}y - \int_D \langle \nabla \wedge \psi, U \rangle \, \mathrm{d}x \\ &= \int_{\partial D} \langle \hat{n} \lrcorner U, \psi \rangle \, \mathrm{d}y, \end{aligned}$$

where we also have used the adjointness between $\wedge$ and $\lrcorner$, i.e., $\langle U, \hat{n} \wedge \psi \rangle = \langle \hat{n} \lrcorner U, \psi \rangle$ (see 2.1). This means that $F = \nabla \lrcorner U$ is orthogonal to $\psi = \nabla \wedge \varphi$ for all functions φ if and only if $\hat{n} \lrcorner U$ on the boundary, which means that $F \in R(\underline{\delta})$. Applying the divergence theorem again, noting that $\int_D \langle \nabla \lrcorner U, \psi \rangle \, \mathrm{d}x = \int_D \langle \nabla \wedge \varphi, F \rangle \, \mathrm{d}x$, and using

the nilpotence of δ, we also get

$$\begin{aligned}\int_D \langle \nabla \wedge \varphi, F\rangle \,\mathrm{d}x &= \int_{\partial D} \langle \hat{n} \wedge \varphi, F\rangle \,\mathrm{d}y - \int_D \langle \varphi, \nabla \lrcorner F\rangle \,\mathrm{d}x \\ &= \int_{\partial D} \langle \hat{n} \wedge \varphi, F\rangle \,\mathrm{d}y \\ &= \int_{\partial D} \langle \varphi, \hat{n} \lrcorner F\rangle \,\mathrm{d}y.\end{aligned}$$

This means that F is orthogonal to $\psi = \nabla \wedge \varphi$ for all functions φ if and only if $\hat{n} \lrcorner F = 0$ on the boundary. Since $\hat{n} \lrcorner F = \hat{n}_1 f_1 + \hat{n}_2 f_2 = \langle \hat{n}, F\rangle$, we conclude that this means that if $F = \nabla \lrcorner U$, then $F \in R(\underline{\delta})$ is equivalent to that F is tangential at the boundary. We note also that the fields in the cohomology space $C_{||}(D)$ are tangential, since $\hat{n} \lrcorner F = 0$ on the boundary for all $F \in C_{||}(D)$. Another remark is that $F = \nabla \lrcorner U$ and $\hat{n} \lrcorner F = 0$ on the boundary are not in general sufficent conditions for concluding $F \in R(\underline{\delta})$. If D is not simply connected, for example if $D = \{(x, y) : 1 < x^2 + y^2 < 4\}$ we can construct a counter example. Let $U = (x^2 + y^2 - 1)e_{12}$. Then $F = \nabla \lrcorner U = -2ye_1 + 2xe_2$ is both divergence free and tangential at the boundary but $F \notin R(\underline{\delta})$, since for points on $x^2 + y^2 = 2$, $\hat{n} \lrcorner U \neq 0$.

To conclude this section, we present the first of two corollaries to Theorem 3.1.6. It is about a different Hodge decomposition, which will not be used in the main parts of this thesis, but it is natural to present for the completeness of this section and its proof is a nice application of the Hodge star maps, contributing to the understanding of computations that will be carried out later. It also involves the space $C_{\perp}(D)$, which like $C_{||}(D)$ is finite dimensional and which is interesting to discuss at the same time as $C_{||}$ in Section 3.2. The second corollary to Theorem 3.1.6 is about uniqueness of potentials, and will be postponed to Section 3.3.

Corollary 3.1.7. ***Normal Hodge decomposition*** *[6, p. 246]*
Let D be a bounded Lipschitz domain in a Euclidean space. Then one has an orthogonal splitting

$$L_2(D) = R(\underline{d}) \oplus C_{\perp}(D) \oplus R(\delta),$$

where $R(\underline{d}) \oplus C_{\perp}(D) = N(\underline{d}), C_{\perp}(D) \oplus R(\delta) = N(\delta)$, $C_{\perp}(D) := N(\underline{d}) \cap N(\delta)$, and the normal cohomology space $C_{\perp}(D)$ is finite-dimensional. At the level of $k-$vector fields, each $L_2(D; \wedge^k V)$ splits in this way.

Proof.

By Theorem 3.1.6, for any $F \in L_2(D)$ one may write $F = F_1 + F_2 + F_3$ with $F_1 \in R(d), F_2 \in C_{||}(D),$ and $F_3 \in R(\underline{\delta})$. This means that

$$F = \nabla \wedge U + F_2 + \nabla \lrcorner V,$$

for some $U, V \in \wedge V$ with $\hat{n} \lrcorner V = 0$ on ∂D. Since this is true for all F, we may as well look at $*F$. Applying the Hodge star to the decomposition above, we get

$$*F = *(\nabla \wedge U) + *F_2 + *(\nabla \lrcorner V) = (*U) \llcorner \nabla + *F_2 + (*V) \wedge \nabla$$

$$= \pm\nabla \lrcorner (*U) + *F_2 - \nabla \wedge (*V) := \tilde{F}_1 + \tilde{F}_2 + \tilde{F}_3,$$

using Proposition 2.3.3, relation d) from Section 2.2, and anticommutativity of the exterior product. We see that $\tilde{F}_1 \in R(\delta)$. Moreover, by using Proposition 2.3.3,

$$\hat{n} \wedge (*V) = -(*V) \wedge \hat{n} = - * (\hat{n} \lrcorner V) = 0 \text{ on } \partial D,$$

since $\hat{n} \lrcorner V = 0$ on ∂D. Therefore, we can conclude $F_3 \in R(\underline{d})$ and by the same reasoning $F_2 \in C_\perp(D)$, thereby proving the corollary. □

One may here also note that the name *normal* Hodge decomposition is due to the fact that the fields in $R(\underline{d})$ are normal to the boundary. By a similar argument as above for the tangential Hodge decomposition, for a field $F \in R(\underline{d}; \wedge^1)$ in a two dimensional domain, one can show that one has $\hat{n} \wedge F = 0$ on the boundary, which is equivalent to $\langle \hat{n}, (*F) \rangle = 0$ on the boundary, which by the observation in Example 2.3.2 implies that F is normal to the boundary (and likewise for the fields in $C_\perp(D)$).

3.2 The cohomology spaces

Now we turn our attention to the *cohomology spaces* $C_{||}(D)$ and $C_\perp(D)$. According to Theorem 3.1.6, $C_{||}(D)$ is finite dimensional and we also have $R(d) \oplus C_{||}(D) = N(d)$. Thus, $C_{||}(D)$ is the gap between $R(d)$ and $N(d)$, and we can find corresponding relations for $C_\perp$. Intuitively, in light of this it is not surprising that the cohomology spaces are smaller than $R(d), R(\underline{d}), R(\delta)$, and $R(\underline{\delta})$. The following definition facilitates a discussion about the dimension of the cohomology spaces.

Definition 3.2.1. [6, p. 244]
Let

$$b_k(D) := \dim(C_{||}(D; \wedge^k)), k = 0, 1, 2, ..., n.$$

The numbers $b_k(D)$ are called the *Betti numbers*.

We assume now that $D = \{(x, y) : x^2 + y^2 < 1\} \subset \mathbb{R}^2$. The conclusions about $\dim(C_{||}(D))$ are valid also for other domains with a similar topology, in particular domains without holes and with a smooth boundary (for details, see [6, p. 373]), but we consider the unit disk for simplicity. Assume further that there is a scalar function $f \in C_{||}(D; \wedge^0)$. By definition of $C_{||}(D)$, one must then have $\nabla \lrcorner f = 0, \nabla \wedge f = 0$, and $\hat{n} \lrcorner f = 0$ on ∂D. The first and third identities are trivially true, since $e_i \lrcorner f = 0$ for all i. The second is true if and only if $\partial_1 f = \partial_2 f = 0$, which in turn is true if and only if f is a constant function. We have thus $b_0(D) = 1$.

Turning the attention to $L_2(D; \wedge^1)$, let F be a vector field. We know from vector calculus that for a simply connected domain D every curl-free vector field is a gradient field. If $F \in C_{||}(D)$, then in particular $dF = 0$, which means F is curl-free (see Example 2.4.3). Therefore we have $F = \nabla U = \partial_1 U e_1 + \partial_2 U e_2$ for some

$U \in L_2(D; \wedge^0)$. The definition of $C_{||}(D)$ also requires $\delta F = 0$, which means $\delta dU = 0$, which is equivalent to $\Delta U = 0$, since

$$\Delta U = (d + \delta)^2 U = (d^2 + d\delta + \delta d + \delta^2)U = \delta dU.$$

Since we also have $\hat{n} \lrcorner F = x\partial_1 U + y\partial_2 U = \nabla U \cdot \hat{n} = 0$ on the boundary for a unit normal $\hat{n} = xe_1 + ye_2$, this means that U is the solution to the Neumann problem

$$\begin{cases} \Delta U = 0 \text{ in } D, \\ \partial_{\hat{n}} U = 0 \text{ on } \partial D. \end{cases}$$

Multiplying with a test function $v \in H^1(D) := \{u(x) \in L_2(D; \wedge^0) : \partial_i u(x) \in L_2(D; \wedge^0),\ i = 1, ..., n\}$ and integrating over the domain, Greens´s theorem gives

$$\int_D \Delta U \cdot v \, \mathrm{d}x = \int_{\partial D} \partial_{\hat{n}} U \cdot v \, \mathrm{d}y - \int_D \nabla U \cdot \nabla v \, \mathrm{d}x = -\int_D \nabla U \cdot \nabla v \, \mathrm{d}x,$$

which leads to the well-known variational formulation to seek $U \in H^1(D)$ such that

$$-\int_D \nabla U \cdot \nabla v \, \mathrm{d}x = 0, \text{ for all } v \in H^1(D).$$

Since this equality should be valid for all $v \in H^1(D)$, we can take $v = U$ and get $-\int_D (\nabla U)^2 \, \mathrm{d}x = 0$ from which one can conclude that $\nabla U = 0$, which means that U is constant and that $F = \nabla U = 0$. We conclude that $C_{||}(D; \wedge^1)$ is empty and thus $b_1(D) = 0$.

Lastly, we assume $F = he_{12} \in C_{||}(D; \wedge^2)$. $\nabla \wedge F = 0$ is trivially true. From $\nabla \lrcorner F = 0$ one can conclude $\partial_1 h = \partial_2 h = 0$, which means that h is constant. From the last part of the definition of $C_{||}(D)$, for an outward pointing unit normal $\hat{n} = xe_1 + ye_2$, one gets

$$\hat{n} \lrcorner F = -yhe_1 + xhe_2 = 0 \text{ on } \partial D.$$

Since we cannot have $x = y = 0$ on the boundary, we must have that $h = 0$ on the boundary. But since h is constant, this means that $h = 0$ in all of D. Thus, $b_2(D) = 0$ and we conclude that $C_{||}(D)$ only contains constant scalar functions and that $\dim(C_{||}(D)) = 1$.

If one instead look at the domain $D = \{(x, y) : 1 < x^2 + y^2 < 2\}$, an annulus, one gets a different result. The vector field $F = (-ye_1 + xe_2)/(x^2 + y^2) \in C_{||}(D; \wedge^1)$ [6, p. 247], which can be verified using Definition 3.0.1. For the annulus, $\dim(C_{||}(D)) = 2$, and one has the Betti numbers $b_0(D) = 1, b_1(D) = 1,$ and $b_2(D) = 0$. In $C_{||}(D; \wedge^0)$ one has the constant scalar functions and $C_{||}(D; \wedge^2) = \{0\}$ for the same reasons as earlier. Looking at the pictures in Figure 3.1 from the beginning of this chapter, one can see that the cohomology part of the decomposed vector field is a field characteristically circulating around the hole of the domain. This will be the case for any decomposition of a vector field with a non-zero cohomology part in a domain with a hole.

As the above discussion indicates, $\dim(C_{\shortparallel}(D))$ contains information about the topology of the domain. The number $b_0(D)$, for example, indicates the number of connected components of D since any function in $C_{\shortparallel}(D)$ has to be constant on each connected component. We end this section by mentioning that the dimension of $C_{\perp}(D)$ can be computed by if one knows the Betti numbers by using $\dim(C_{\perp}(D;\wedge^k)) = b_{n-k}(D)$ [6, p. 373]. The dimension of this cohomology space also contains topological information, but since we will not use the normal Hodge decompositions in the computations in Chapter 4 of this thesis, we do not present the details.

3.3 Hodge decompositions and PDE:s

The main application of Hodge decompositions in this thesis is to use the tangential Hodge decomposition to solve the Stokes equation under the Hodge boundary conditions. In this section, the link between Hodge decompositions and partial differential equations (PDE:s) will be explained by two examples highlighting how the Hodge decompositions give existence and uniqueness results for solutions to the Poisson equation [6][pp. 249ff]. We start this section by presenting a second corollary to Theorem 3.1.6. In general, potentials U such that $F = \nabla \wedge U$ or $F = \nabla \lrcorner U$ are not unique. For example, if U is a scalar function one has $\nabla \wedge U = \nabla U = \nabla(U + C_1) = \nabla \wedge (U + C_1)$ for any constant C_1. In the same way, if $U = fe_1 + ge_2$ is a vector valued function, then $\nabla \lrcorner (fe_1 + ge_2) = \partial_1 f + \partial_2 g = \nabla \lrcorner ((f + f_1(y))e_1 + (g + g_1(x))e_2)$ for any scalar functions of one variable $f_1(y)$ and $g_1(x)$. Under some conditions, though, one can find unique potentials, and that is the content of the following corollary.

Corollary 3.3.1. *[6, pp. 246f]*
We have the following uniqueness results for potentials.

a) $\forall F \in R(d)$, $\exists!\ U \in R(\underline{\delta})$ *such that* $F = \nabla \wedge U$,
b) $\forall F \in R(\underline{d})$, $\exists!\ U \in R(\delta)$ *such that* $F = \nabla \wedge U$,
c) $\forall F \in R(\delta)$, $\exists!\ U \in R(\underline{d})$ *such that* $F = \nabla \lrcorner U$, *and*
d) $\forall F \in R(\underline{\delta})$, $\exists!\ U \in R(d)$ *such that* $F = \nabla \lrcorner U$.

Proof.

We show it for a), the other cases are proven in the same way.

a) Let $F = \nabla \wedge U$. Using tangential Hodge decomposition (Theorem 3.1.6), we can write

$$U = U_1 + U_2 + U_3, \text{ with } U_1 \in R(d), U_2 \in C_{\shortparallel}(D), \text{ and } U_3 \in R(\underline{\delta}).$$

Moreover, $\nabla \wedge U_1 = 0$, by nilpotence of d (see Section 2.4), and $\nabla \wedge U_2 = 0$, since $C_{\shortparallel}(D) \subset N(d)$. By Theorem 3.1.3, $R(\underline{\delta})$ is a closed subspace, and since $R(d) \oplus C_{\shortparallel}(D) = N(d)$ and thus $R(\underline{\delta})^{\perp} = N(d)$, Theorem 3.1.2 gives that $U = U_3$ is the unique potential $U \in R(\underline{\delta})$ such that $\nabla \wedge U = F$. □

Consider the Poisson equation with homogeneous Dirichlet boundary conditions

$$\begin{cases} \Delta u(x) = g(x), \text{ for } x \in D, \\ u(x) = 0, \text{ for } x \in \partial D, \end{cases}$$

where we seek $u(x) \in H_0^1(D) := \{u(x) \in H^1(D) : u(x)|_{\partial D} = 0\}$ and where $g(x) \in L_2(D; \wedge^0)$ is a given scalar function. Since $u(x) \in L_2(D; \wedge^0)$ is a scalar function, we have $\delta u(x) = 0$ and thus $\Delta u(x) = \delta d u(x)$. The above is therefore equivalent to

$$\begin{cases} \delta d u(x) = g(x), \text{ for } x \in D, \\ u(x) = 0, \text{ for } x \in \partial D. \end{cases}$$

Using the relations between the interior and exterior derivative and the gradient and divergence described in Example 2.4.3, one may rewrite the first equation as

$$\begin{cases} \operatorname{div}(F) = g(x), \\ \nabla u(x) = F. \end{cases}$$

Since we are searching for a function $u(x)$ with $u(x)|_{\partial D} = 0$, we can conclude that $F \in R(\underline{d})$. By the normal Hodge decomposition and Corollary 3.3.1c), there is a unique $F \in R(\underline{d})$ such that $g(x) = \nabla \lrcorner F = \operatorname{div}(F)$. Using b) from the same corollary gives that there is a unique $u(x) \in R(\delta)$ such that $\nabla \wedge u(x) = \nabla u(x) = F$. Since $C_\perp(D; \wedge^0)$ and $R(\underline{d}; \wedge^0)$ both are empty, the normal Hodge decomposition gives that this $u(x)$ is the unique solution to the above Poisson equation.

Consider now the Poisson equation with homogeneous Neumann boundary conditions

$$\begin{cases} \Delta u(x) = g(x), \text{ for } x \in D, \\ \partial_{\hat{n}} u(x) = 0, \text{ for } x \in \partial D, \end{cases}$$

with $g \in L_2(D; \wedge^0)$ and where we now seek $u(x) \in H^1(D)$. By the same reasoning as above, the first equation may be rewritten as

$$\begin{cases} \operatorname{div}(F) = g(x), \\ \nabla u(x) = F. \end{cases}$$

Using instead the tangential Hodge decomposition and Corollary 3.3.1d), we get that there is a unique $F \in R(d)$ such that $g(x) = \operatorname{div}(F)$, if we demand that $g(x) \in R(\underline{\delta})$, which means that $g(x)$ must be orthogonal to $C_{||}(D)$, that is, orthogonal to the functions that are constant on each connected component of D (see Section 3.2). Moreover, by Corollary 3.3.1a), $u(x)$ is the unique scalar function in $R(\underline{\delta})$ such that $\nabla u(x) = F$. As opposed to the case with Dirichlet boundary conditions, this $u(x)$ is not the unique solution in $L_2(D; \wedge^0)$, though, since $C_{||}(D; \wedge^0)$ is not empty but consists of the componentwise constant scalar functions. Thus, the solution $u(x)$ is only unique if we demand that it should be orthogonal to $C_{||}(D)$.

3.4 Algorithm for computing a Hodge decomposition

Computing the tangential Hodge decomposition of a vector field $F \in L_2(D; \wedge^1)$, with $D \subset \mathbb{R}^2$, is an essential part of solving the Stokes equation in Section 4.2. In this section, an algorithm that can be used to numerically compute this decomposition is described. The algorithm follows Rosén [6, pp. 248f]. It uses the finite element method (FEM), which is also briefly explained in this section. For a more rigorous depiction of FEM, see e.g. [1, 7]. The MATLAB code used to implement the algorithm, creating the plots in this section, can be found in appendix A.

Let $F \in L_2(D; \wedge^1)$, for a $D \subset \mathbb{R}^2$, be a given vector field. We want to compute the tangential Hodge decomposition, that is, we want to decompose $F = F_1 + F_2 + F_3$ where $F_1 \in R(d), F_2 \in C_{||}(D)$, and $F_3 \in R(\underline{\delta})$. To do this, one has to seek scalar functions U and V such that $F_1 = \nabla \wedge U = \nabla U$ and $F_3 = \nabla \lrcorner Ve_{12}$. Since $F_3 \in R(\underline{\delta})$, we should have $\hat{n} \lrcorner Ve_{12} = 0$ on ∂D. If we let $\hat{n} = \hat{n}_1 e_1 + \hat{n}_1 e_2$, we see that $\hat{n} \lrcorner Ve_{12} = -\hat{n}_2 Ve_1 + \hat{n}_1 Ve_2$ and that this equals zero on ∂D exactly when $V|_{\partial D} = 0$. In the same way, since $C_{||}(D) \subset N(\underline{\delta})$, we have $F_2|_{\partial D} = 0$.

To find U, one uses that $F - \nabla U \in N(\underline{\delta})$, since $N(\underline{\delta}) = C_{||}(D) \oplus R(\underline{\delta})$ by Theorem 3.1.6. This is equivalent to saying that $F - \nabla U$ is orthogonal to $R(d)$, i.e., $\langle F - \nabla U, \nabla \Phi \rangle = 0$ for any $\Phi \in H^1(D)$, which is equivalent to $\langle \nabla U, \nabla \Phi \rangle = \langle F, \nabla \Phi \rangle$. Integrating this over the domain D, one gets the variational equations

$$\text{seek } U \in H^1(D) \text{ such that } \int_D \langle \nabla U, \nabla \Phi \rangle \, \mathrm{d}x = \int_D \langle F, \nabla \Phi \rangle \, \mathrm{d}x, \text{ for all } \Phi \in H^1(D).$$

This can be solved using *the finite element method* (FEM), where one discretizes the equation in order to find an approximate solution. To be able to discretize the equation, one has to replace the function space $H^1(D)$ with a finite-dimensional subspace. This can be done in several ways, but we present here one of the standard methods for two dimensional domains. First one divides the domain D into smaller parts by a triangulation. This can be made for example using the application pdeModeler in MATLAB. The picture below, Figure 3.2, shows a triangulation of the unit disk.

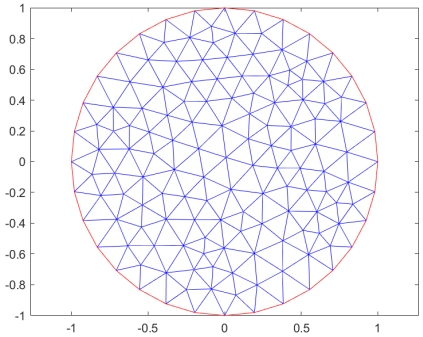

Figure 3.2: A mesh for the unit disk which can be used for implementing the finite element method. A finer mesh gives a more accurate approximation.

Thereafter, one defines a basis for a finite-dimensional subspace $U_h \subset H^1(D)$. The basis functions are often chosen to be piecewise linear, and in such a way that they equal one on one node and zero on all other nodes. These functions are sometimes called tent functions, see the picture below for an example.

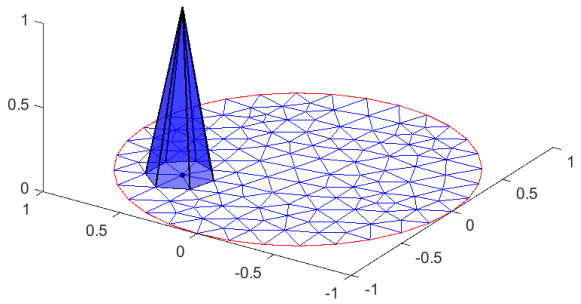

Figure 3.3: An example of a basis function $\psi \in U_h$. Note that it is piecewise linear and equals one on the marked node, but zero on all other nodes.

The basis of the N-dimensional function space U_h is now taken to be $\{\psi_1, \psi_2, ..., \psi_N\}$, where each ψ_i is piecewise linear and equals one on node i and zero on all other nodes. The discrete analogue of the equation to be solved is now

$$\text{seek } u_h \in U_h \text{ such that } \int_D \langle \nabla u_h, \nabla \psi \rangle \, \mathrm{d}x = \int_D \langle F, \nabla \psi \rangle \, \mathrm{d}x, \text{ for all } \psi \in U_h.$$

The approximate solution to the partial differential equation is then obtained by the ansatz

$$U \approx u_h = \sum_i^N \zeta_i \psi_i,$$

where ζ_i are the coefficients one is looking for. Putting this into the equation and letting the ψ:s vary over the basis functions, this leads to a system of equations

$$\sum_i^N \sum_j^N \left(\int_D \langle \nabla \psi_i, \nabla \psi_j \rangle \, \mathrm{d}x \right) \zeta_i = \sum_i^N \int_D \langle F, \nabla \psi_i \rangle \, \mathrm{d}x,$$

which one usually writes in short form $A\boldsymbol{\zeta} = b$, where $1 \leq i \leq N$, and

$$A = (a_{ij}) = \int_D \langle \nabla \psi_i, \nabla \psi_j \rangle \, \mathrm{d}x,$$

$$\boldsymbol{\zeta} = (\zeta_i) = \zeta_i, \text{ and}$$

$$b = (b_i) = \int_D \langle F, \nabla \psi_i \rangle \, \mathrm{d}x.$$

The solution of this system of equations give the coefficients in $\boldsymbol{\zeta}$, and one has thereby computed an approximation of U.

The next step to compute the tangential Hodge decomposition is to compute V. To do that, one can begin by using the Hodge star maps as described in Example 2.3.2 and relation d) from Section 2.2. This leads to similar variational equations for V as for U. To see this, compute

$$\begin{aligned}
*F &= *(\nabla U) + *F_2 + *(\nabla \lrcorner V e_{12}) \\
&= e_{12} \llcorner (\partial_1 U e_1 + \partial_2 U e_2) + *F_2 + e_{12} \llcorner (-\partial_2 V e_1 + \partial_1 V e_2) \\
&= -(\partial_1 U e_1 + \partial_2 U e_2) \lrcorner e_{12} + *F_2 + (\partial_2 V e_1 - \partial_1 V e_2) \lrcorner e_{12} \\
&= -\partial_1 U e_2 + \partial_2 U e_1 + *F_2 + \partial_2 V e_2 + \partial_1 V e_1 \\
&= \nabla V + *F_2 - \nabla \lrcorner U e_{12}.
\end{aligned}$$

Reasoning as before, we now have $\langle \nabla V, \nabla \Phi \rangle = \langle *F, \nabla \Phi \rangle$, which leads to the variational equations

$$\text{seek } V \in H_0^1(D) \text{ such that } \int_D \langle \nabla V, \nabla \Phi \rangle \, \mathrm{d}x = \int_D \langle *F, \nabla \Phi \rangle \, \mathrm{d}x, \text{ for all } \Phi \in H_0^1(D),$$

where one imposes the Dirichlet boundary condition on V by using the space $H_0^1(D)$.

Lastly, when U and V are computed, one can just set $F_2 = F - \nabla U - \nabla \lrcorner V e_{12}$, and the decomposition of F is done.

Below are some plots of a tangential Hodge decomposition of a vector field F[3] in a simply connected domain.

[3] $F = (-2x(1-x^2-y^2) + 4xy^2 + 2xy - 3x^2y^2)e_1 + (2y(1-x^2-y^2) - 4x^2y + x^2 - 2x^3y)e_2$.

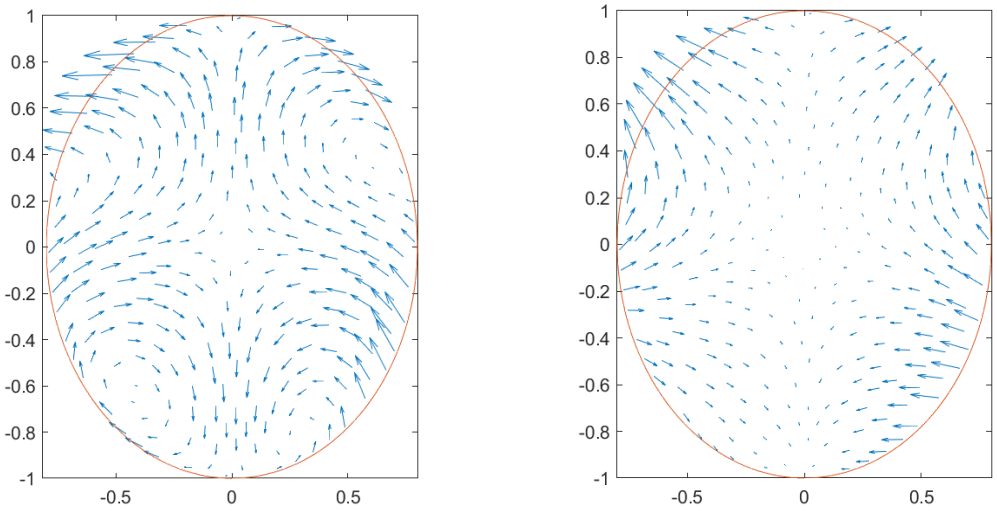

(a) The vector field F.

(b) $F_1 = \nabla U$.

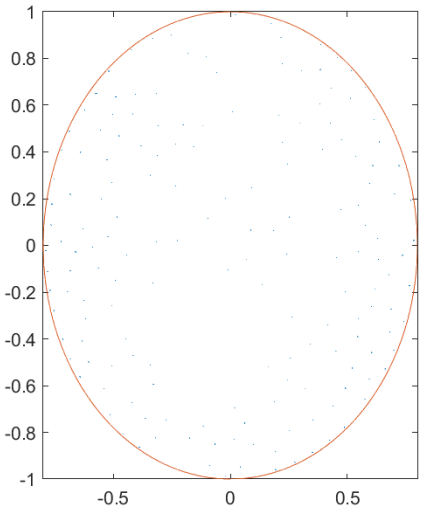

(c) F_2.

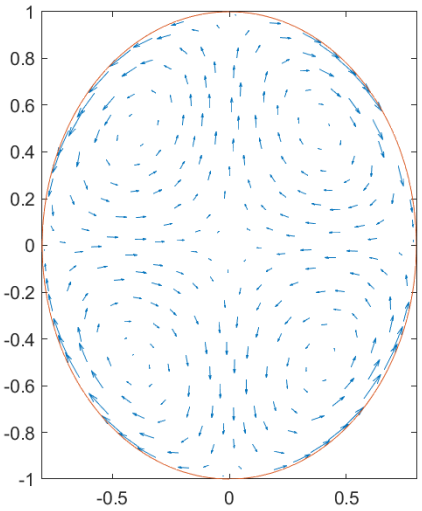

(d) $F_3 = \nabla \lrcorner Ve_{12}$.

Figure 3.4: Example of a tangential Hodge decomposition, $F = F_1 + F_2 + F_3$. All plots are made in the same scale. F is in this example chosen in such a way that both F_1 and F_3 are substantial contributors to F. F_2 always equals zero for vector fields in simply connected domains.

Note that the gradient field F_1 is curl free and that F_3 is divergence free, which can be seen directly from Theorem 3.1.6 since d and δ are nilpotent operators, applying the observations from Example 2.4.3. Geometrically, one can see that the gradient vector field gives information about the potential U. Since the gradient points at the direction where the function is growing fastest, one can for example see that U increases a lot at the top left parts of the domain. The divergence free field is recognized by the fact that the flow into a small region should equal the flow out from that region. In Figure 3.4 we see that F_2 rotates around certain points where the vector lengths seems to depend on the distance to the center of rotation. Since the domain D in this case is just an ellipse without holes we have $C_{||}(D; \wedge^1 V) = \{0\}$ (see Section 3.2), which can be compared to the pictures in Figure 3.1. The small

dots that can be seen in the picture above for F_2 are due to computational errors. Recall that a vector field in $C_{||}(D)$ should be both curl free and divergence free as well as tangential at the boundary. If one has a hole in the domain, as in Figure 3.1, these requirements can be met by a field rotating around the hole. One can think of the center of rotation as being in that hole, but the curl in the domain can still be zero since the points in the hole is outside the domain.

CHAPTER 4

Solving the Stokes equation

The main goal of this project is to solve and try to understand the Stokes equation with Hodge boundary conditions. This chapter starts by a short general introduction of the Stokes equation, followed by two sections where the Stokes equation is solved under different boundary conditions. In Section 4.2 the Hodge boundary conditions are used and interpreted, which leads to the main results of this thesis. In Section 4.3 the more standard no-slip boundary condition is used.

4.1 The Stokes equation

The Stokes equation describes the flow of an incompressible, viscous fluid. A typical example of such a flow would be honey or syrup. In this section, some of the theory behind the Stokes equation will be briefly explained.

The fundamental partial differential equations that describes fluids stem from the physical laws considering conservation of mass and conservation of momentum [7, p. 142]. In fluid mechanics, the law of conservation of mass can be expressed

$$\partial_t \rho + \operatorname{div}(\rho v) = 0,$$

where ρ is the density, t the time, and v the flow velocity field. If one considers incompressible fluids, then the density ρ is constant. The above equation then becomes

$$\rho \operatorname{div}(v) = 0,$$

which means that $\operatorname{div}(v) = 0$. Newton's law for conservation of momentum states that the rate of change of momentum of a particle equals the sum of the forces acting on the particle. In the case of fluids in a fixed region, there are four different contributors to the sum of the forces: the flow of momentum into the region, the pressure, the viscous forces, and the external forces (for example gravity). This leads to the following equation

$$\rho(\partial_t v + \partial_v v) = -\nabla p + \mu \Delta v + f,$$

where p is the pressure, μ is a constant measuring the viscosity, and f represents external forces. The above equation is a non-linear equation, but if one makes some additional assumptions, one can get a linear equation. If one assumes that

the velocity at every point is constant, the term $\partial_t v$ vanishes. Moreover, the most difficult term, $\partial_v v = (v \cdot \nabla)v$, can be neglected when considering small velocities. With these simplifications, one has arrived at the Stokes equation for viscous flows, which can be formulated

$$\begin{cases} \nabla p - \mu \Delta v = f, \\ \operatorname{div}(v) = 0. \end{cases}$$

In the following two sections solutions to this equation under different boundary conditions will be presented. The first boundary conditions, in Section 4.2, are, given the theory of Hodge decompositions, a natural choice of boundary conditions from a mathematical point of view. They are, though, non-physical. The no-slip boundary condition, used in Section 4.3, is supported by empirical facts, but it leads to a more involved mathematical treatment of the equations than the Hodge boundary conditions.

4.2 The Hodge boundary conditions

In this section an algorithm for numerically solving the Stokes equation under the Hodge boundary conditions will be described. The algorithm is basically an application of the tangential Hodge decomposition described in Section 3.1. For simplicity, the domain is in this section taken to be simply connected. As a remark, the theory below works in other cases too, given that the input f is orthogonal to $C_{\shortparallel}(D)$. In appendix A one can find the full MATLAB code used for implementing this algorithm and making the plots below. The Hodge boundary conditions consists of two parts. The boundary condition on v is just a tangential condition, which means that the restriction on the flow of the fluid is that it may not cross the boundary (e.g. the bottle keeping the fluid inside). The second condition is imposed on the vorticity $\omega = dv$. In line with the theory of Hodge decompositions, the condition is that $\hat{n} \lrcorner \omega = \hat{n} \lrcorner (dv) = 0$ on the boundary. In three dimensions, this would mean that the bivector field ω is tangential or equivalently that the vector field $*\omega$ is normal to the boundary. In our case, dealing with a two dimensional domain, this simplifies to $\omega|_{\partial D} = 0$. To see this, letting $\omega = \omega e_{12}$ and $\hat{n} = \hat{n}_1 e_1 + \hat{n}_2 e_2$, note that

$$\hat{n} \lrcorner \omega e_{12} = -\hat{n}_2 \omega e_1 + \hat{n}_1 \omega e_2,$$

and that this equals zero on the boundary if and only if $\omega|_{\partial D} = 0$. In summary, for a two-dimensional domain we formulate the problem in this section as

$$\begin{cases} \nabla p - \mu \Delta v = f, \text{ in } D, \\ div(v) = \delta v = 0, \text{ in } D, \\ \hat{n} \cdot v = 0, \text{ on } \partial D, \\ \omega = dv = 0, \text{ on } \partial D. \end{cases} \tag{4.1}$$

Since μ is only a constant, for simplicity we consider the case $\mu = 1$. We begin by rewriting the left hand side of the first equation as

$$\nabla p - \Delta v = \nabla p - (d + \delta)^2 v = \nabla p - \delta dv,$$

since $d\delta v = 0$, using the second equation. Letting $\omega' = -\omega = -dv$ one may again rewrite the first equation to

$$\nabla p + \delta\omega' = f,$$

where $\omega' \in \wedge^2 D$ with $\omega'|_{\partial D} = 0$. The scalar function p and the bivector field $\omega' = \omega' e_{12}$ can now be found by a tangential Hodge decompoisition, using the method described in Section 3.4 applied to the given vector field f. By just changing the sign on ω', since $\omega' = -\omega$, we also have ω. Moreover, since $v \in L_2(D; \wedge^1)$ and $C_{||}(D; \wedge^1) = \{0\}$ for a simply connected domain, by the tangential Hodge decomposition and $\operatorname{div}(v) = 0$ we conclude that $v \in R(\underline{\delta})$ and let $v = \delta\varphi e_{12}$, with $\varphi e_{12} \in R(d)$. We may thus write

$$\delta\omega' e_{12} = \delta d\delta\varphi e_{12},$$

which is equivalent to

$$\omega' e_{12} = (\Delta\varphi) e_{12},$$

since $\Delta\varphi = (d+\delta)^2\varphi = d\delta\varphi$. By applying the (left or right) Hodge star map, one can rewrite this as

$$\Delta\varphi = \omega',$$

considering φ and ω' as scalar functions. This equation looks like the Poisson problem, but to compute the solution one needs a boundary condition. First we note that φe_{12} is the unique potential in $R(d)$ such that $v = \delta\varphi e_{12}$ by Corollary 3.3.1d). Moreover, since $v \in R(\underline{\delta})$ implies that $\hat{n} \lrcorner \varphi e_{12} = -\hat{n}_2\varphi e_1 + \hat{n}_1\varphi e_2 = 0$ on ∂D, we can conclude $\varphi|_{\partial D} = 0$ since if there would be a point on the boundary where $\varphi \neq 0$, then $\hat{n}_1 = \hat{n}_2 = 0$ at this point which is not possible. This means that we can formulate the Poission equation with homogeneous Dirichlet boundary conditions:

$$\begin{cases} \Delta\varphi = \omega', \text{ in } D, \\ \varphi = 0, \text{ on } \partial D. \end{cases}$$

Solving this equation gives the scalar function φ, and lastly one can compute v by setting $v = \delta(\varphi e_{12})$.

Below are some plots showing solutions to the Stokes equation with the Hodge boundary conditions.

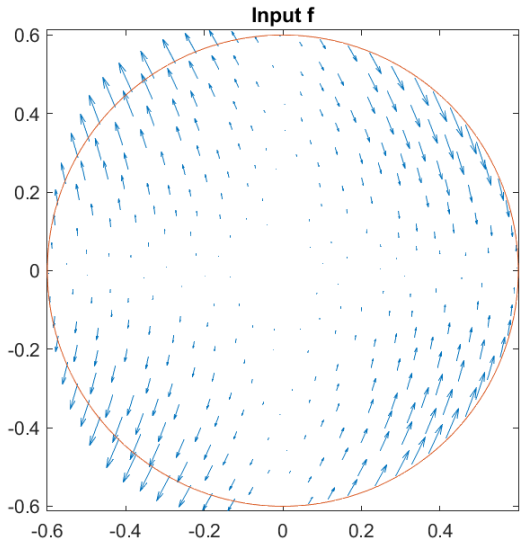

(a) The external force f.

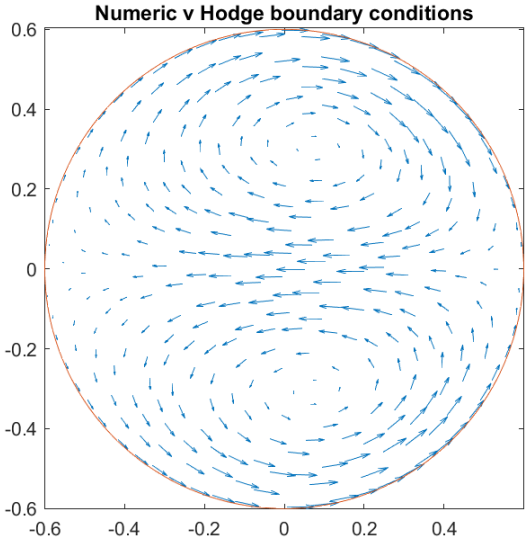

(b) The velocity field v.

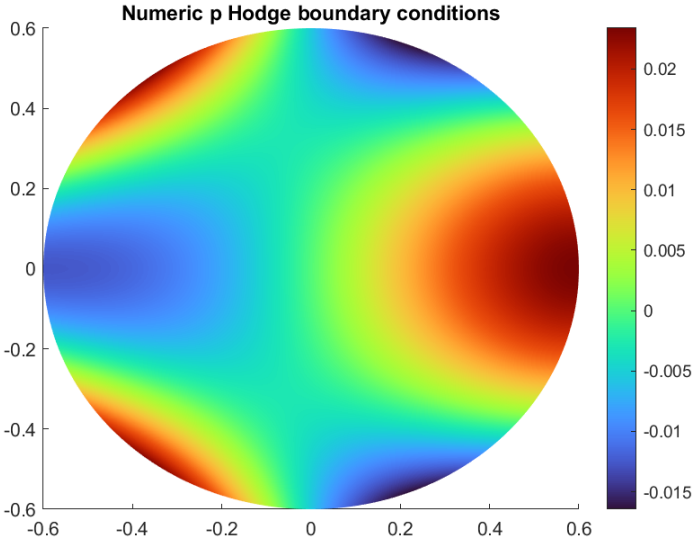

(c) The pressure p.

Figure 4.1: Solution to the Stokes equation with Hodge boundary conditions (4.1). The field $f = xy^2e_1 - xye_2$ is plotted with the in-built autoscale function of the MATLAB command 'quiver'. The vector field v, where the vectors are substantially smaller, is scaled with the factor 50.

As can be seen in the pictures above, the Hodge boundary conditions allow the liquid to slip, contrary to the empirical fact that viscous flows stick to the boundary. The external forces points out of the boundary in some places, and those regions are the ones with higher pressure. Since v is not allowed to pass through the boundary, the velocity fields bends and becomes tangential. To the right of the domain, close to the boundary, the external forces point at opposite directions. This is the region with the highest pressure, and the forces cause the velocity field to flow to the left. The result is two swirls in the field.

One may ask how the Hodge boundary conditions should be interpreted in a more rigorous way, and in particular what happens to the flow at the boundary. Below are some plots showing the size (length) of the vectors in the numerically computed vector field v for different domains but the same input f.

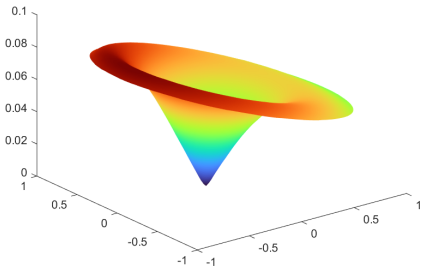

(a) Vector lengths of v where D is the unit disk, 3D-view.

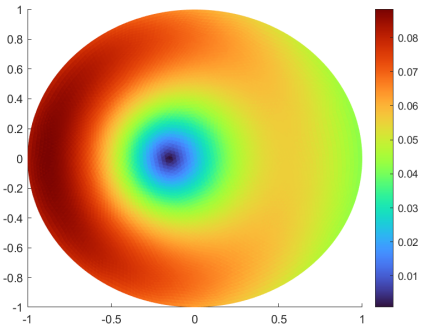

(b) Vector lengths of v where D is the unit disk, 2D-view.

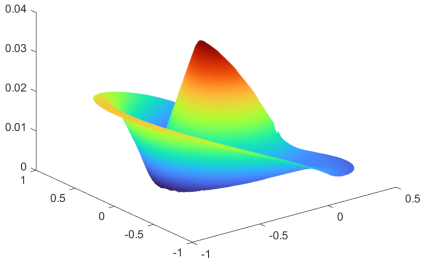

(c) Vector lengths of v where D is a "C-shaped" domain, 3D-view.

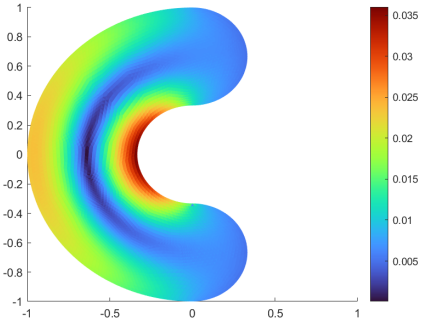

(d) Vector lengths of v where D is a "C-shaped" domain, 2D-view.

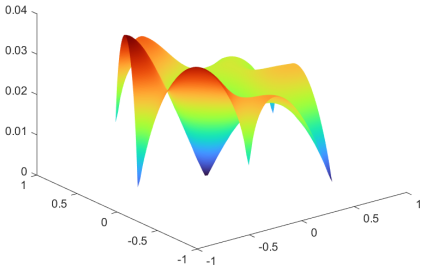

(e) Vector lengths of v where D is a polygonal domain, 3D-view.

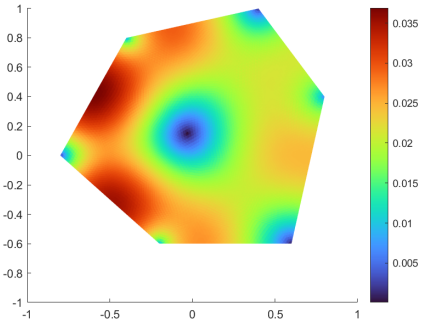

(f) Vector lengths of v where D is a polygonal domain, 2D-view.

Figure 4.2: Vector lengths for the tangential field v in the Stokes equation for different domains D. The plots show vector lengths for three different domains. The same input function $f = (x + y)e_1 + (x^2 - y^2)e_2$ has been used to produce the plots and the 3D-plots are made by interpolating triangular data.

Looking at the plots for the unit circle, Figure 4.2a) and b), one can see that if one starts at a point in the domain and thereafter moves orthogonally towards the boundary (i.e., when one studies the normal derivative) the vector lengths seem to decrease a bit close to the edge. On the pictures it looks like the way the vector length is decreasing is similar all around the boundary. In some way, even though the fluid is allowed to slip at the boundary, it appears that it slows down a bit when getting close to the boundary. Looking at the two pictures in the middle of Figure 4.2, c) and d), it seems that the largest decreasing in vector lengths takes place at the top right and bottom right parts of the 2D-view. One can also see that on the non-convex part of the boundary, the vector lengths instead increase when moving orthogonally towards the boundary. In the last two pictures, Figure 4.2 e) and f), one sees a dramatic drop when getting close to a corner. This is not so surprising when v is supposed to be tangential at the boundary. When moving from a point orthogonally towards a boundary point not very close to a corner, one does not see the pattern of decreasing, or increasing, vector lengths as in the other domains of Figure 4.2. These six pictures together suggest that the normal derivative of the vector lengths in v close to the boundary is in some way determined by the geometry of the domain. We shall see that this is indeed the case.

To be able to investigate further what happens to the vector lengths close to the boundary, we begin by introducing a notion of *curvature*. The curvature at a point on the boundary gives a measure of how much the boundary bends at that point. A convex part of the boundary has a positive curvature, and when the boundary bends a lot the curvature is large. A non-convex part on the other hand has a negative curvature. For a point $P = (x_1, y_1)$ on the boundary, the curvature can be defined in the following way[1]. First, identify the point P as the origin of a coordinate system, and define e_2 in such a way that $\hat{n} = -e_2$ for the unit normal vector $\hat{n}$ at P. Let e_1 be orthogonal to e_2, tangential to the boundary. The following picture, Figure 4.3, describes the setup.

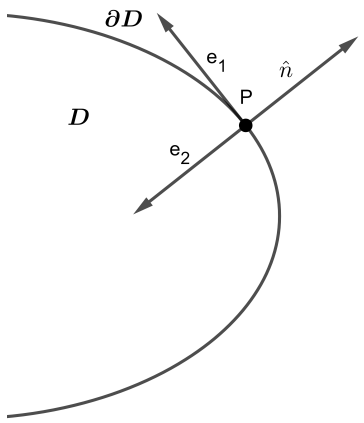

Figure 4.3: Setup for defining the curvature of the boundary.

[1]The definition agrees with the *Weingarten map*, see for example [6, pp. 356f].

Letting e_1 and e_2 be fixed as in Figure 4.3, the *curvature* k at P, counter-clockwise, can be defined by $ke_1 := \partial_1 \hat{n}$ or equivalently $k := e_1 \lrcorner (\partial_1 \hat{n}) = \partial_1 \hat{n}_1$. We will not need to explicitly compute the curvature, but the intuition behind the definition is that when P moves counter-clockwise on ∂D, then the rate at which the e_1-part of $\hat{n}$ changes measures how much the boundary bends. Below is a picture describing the curvature at two different points at the boundary for the domain of Figure 4.2 c) and d) above.

Example 4.2.1.

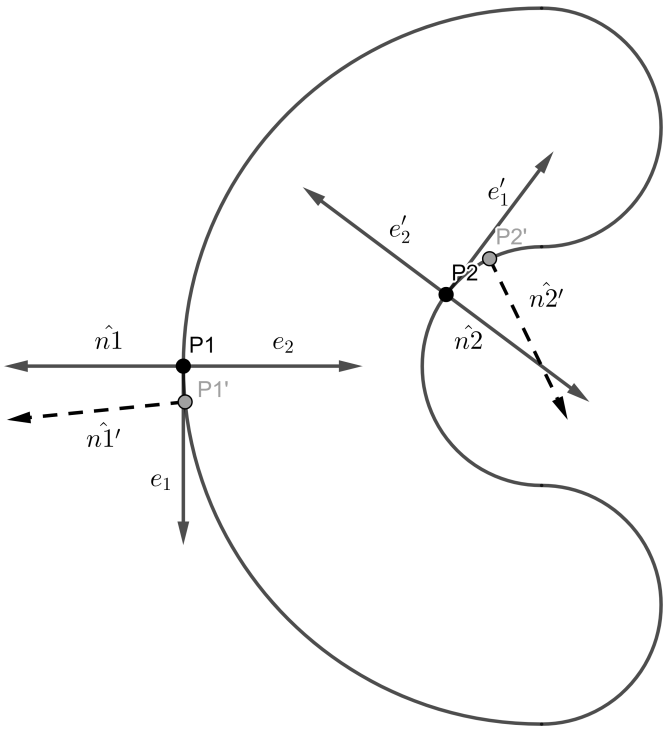

Figure 4.4: The domain of Figure 4.2 c) and d), with the same setup as in Figure 4.3 for two different points.

The boundary of the domain is to the left defined by half a unit circle, and to the right by three half circles with radius $\frac{1}{3}$. Note that the curvature is constant on a circle.

When moving the point $P1$ counter-clockwise along the boundary, the normal vector moves towards e_1 or, more precisely, the angle between the normal vector and e_1 decreases. This corresponds to a positive curvature. At point $P2$, the

opposite situation occurs; the angle between the normal vector and e_1' increases. In this case, the curvature is negative. The largest value of the curvature in the domain is on the small half-circles at the top right and bottom right parts.

With the concept of curvature defined in this way, we shall soon see that the Hodge boundary conditions can be seen as a special case of another set of boundary conditions which are sometimes used when solving the Stokes equation instead of the no-slip boundary condition presented in detail in the next section. They are called the *Navier's slip boundary conditions* after Claude-Louis Navier [5] and can be formulated as follows

$$\begin{cases} v \cdot \hat{n} = 0 \text{ on } \partial D, \\ 2[D(v)\hat{n}]_\tau + \alpha v_\tau = 0 \text{ on } \partial D, \end{cases}$$

where $D(v) := \frac{1}{2}(\nabla v + \nabla v^T)$, $[\cdot]_\tau$ denotes the tangential component of a vector at the boundary and α is a scalar function describing the friction, where one typically has $\alpha \geq 0$ ($\alpha = 0$ denotes a situation with no friction at all). As mentioned earlier, observations suggests that a viscous fluid sticks to the boundary, or, at least, it *almost* sticks. The Navier's slip boundary conditions can be used in the case where a small slip at the boundary is allowed. This corresponds to saying that α, which is determined by properties of the material of the boundary, is large.

The link between the Hodge boundary conditions and the Navier's slip conditions is interesting, and has been discussed in [4]. As it turns out, for the Hodge boundary conditions in a two-dimensional domain, one can translate the concept of curvature at the boundary to the friction function in Navier's slip conditions. With the Hodge boundary conditions, we assume $\hat{n} \cdot v = 0$ for all points on the boundary. Thus, we know that

$$\partial_1(\hat{n} \cdot v) = 0.$$

Expanding the left hand side, letting $v = v_1 e_1 + v_2 e_2$, we get

$$\begin{aligned} \partial_1(v \cdot \hat{n}) &= \partial_1 \hat{n} \cdot v + \hat{n} \cdot \partial_1 v \\ &= k e_1 \cdot v - e_2 \cdot \partial_1 v \\ &= k v_1 - \partial_1 v_2, \end{aligned}$$

and thus

$$k v_1 - \partial_1 v_2 = 0,$$

or equivalently

$$\partial_1 v_2 = k v_1. \tag{4.2}$$

Moreover, since $\omega = dv = (\partial_1 v_2 - \partial_2 v_1) e_{12} = 0$ on the boundary, we have that

$$\partial_2 v_1 = \partial_1 v_2,$$

and, combining this with equation 4.2 above,

$$\partial_2 v_1 = k v_1. \tag{4.3}$$

With the above observations, by adding equations 4.2 and 4.3 and dividing with two, we can conclude that the Hodge boundary conditions are equivalent to

$$\frac{1}{2}(\partial_2 v_1 + \partial_1 v_2) = k v_1.$$

This can be compared to the Navier's slip boundary conditions mentioned above. With the same setup as showed in Figure 4.3, we would get

$$2[D(v)\hat{n}]_\tau + \alpha v_\tau = 0$$

$$\Leftrightarrow 2\left[\frac{1}{2}\left(\begin{bmatrix}\partial_1 v_1 & \partial_2 v_1\\ \partial_1 v_2 & \partial_2 v_2\end{bmatrix} + \begin{bmatrix}\partial_1 v_1 & \partial_1 v_2\\ \partial_2 v_1 & \partial_2 v_2\end{bmatrix}\right)\begin{bmatrix}0\\-1\end{bmatrix}\right]_\tau + \alpha v_1 = 0$$

$$\Leftrightarrow \begin{bmatrix}-(\partial_2 v_1 + \partial_1 v_2)\\ -2\partial_2 v_2\end{bmatrix}_\tau + \alpha v_1 = 0$$

$$\Leftrightarrow \frac{1}{2}(\partial_2 v_1 + \partial_1 v_2) = \frac{\alpha}{2} v_1.$$

From this, we see that the Hodge boundary conditions are equivalent to the Navier´s slip boundary conditions where $\alpha = 2k$, that is α only depends on the curvature of the boundary. Since the curvature, and therefore also the friction at the boundary, is constant on a circle, this fits well with the earlier observation below Figure 4.2 of the vector lengths close to the boundary in the unit disk. It also means that the friction is zero at the edges of the polygon in Figure 4.2e) and f), allowing a "perfect slip". We conclude this section by also mentioning that the Navier's slip boundary conditions are related to the Robin boundary conditions. For a scalar equation, the homogeneous Robin boundary condition reads

$$\beta u + \gamma \partial_{\hat{n}} u = 0, \text{ on } \partial D,$$

where u is the scalar function one seeks and β and γ are constants (or given scalar functions). Using our setup as in Figure 4.3 and the Hodge boundary conditions, we can rewrite equation 4.3 as

$$k v_1 + \partial_{\hat{n}} v_1 = 0,$$

since $\hat{n} = -e_2$. This can be viewed as a homogeneous Robin boundary condition imposed on the scalar function v_1.

4.3 The no-slip boundary condition

It is a well-known empirical fact that viscous flows in e.g. a bottle tend to stick to the boundary. This motivates the following standard formulation of the Stokes equation

$$\begin{cases} \nabla p - \mu \Delta v = f, \text{ in } D, \\ \operatorname{div}(v) = \delta v = 0, \text{ in } D, \\ v = 0, \text{ on } \partial D. \end{cases} \tag{4.4}$$

The boundary condition $v = 0$, on ∂D will be referred to as the *no-slip boundary condition*. In this section an algorithm for solving this problem using the finite element method will be presented, and again the full MATLAB code used to implement it and to make the plots below can be found in the appendix A. The algorithm involves a mixed finite element method and roughly follows Johnson [3, pp. 232f; p. 237]. Again, for simplicity, we consider the case where $\mu = 1$.

To get a variational formulation of the above problem, we define the function spaces

$$V := H_0^1(D) \times H_0^1(D), \text{ and}$$

$$H := L_2(D).$$

We start by multiplying the first equation by $\psi \in V$ and integrating over the domain. Note here that $\psi = (\psi_1, \psi_2)$. Rewriting the left hand side with the help of the Divergence theorem as in 3.1 and Green's theorem as in Section 3.2, and thereafter using the boundary condition, one gets

$$\begin{aligned} \int_D (\nabla p - \Delta v) \cdot \psi \, \mathrm{d}x &= \int_{\partial D} p\hat{n} \cdot \psi \, \mathrm{d}y - \int_D p(\operatorname{div}(\psi)) \, \mathrm{d}x - \left(\int_{\partial D} \partial_{\hat{n}} v \cdot \psi \, \mathrm{d}y - \int_D \nabla v \cdot \nabla \psi \, \mathrm{d}x \right) \\ &= \int_D \nabla v \cdot \nabla \psi - p(\operatorname{div}(\psi)) \, \mathrm{d}x, \end{aligned}$$

and thus one has

$$\int_D \nabla v \cdot \nabla \psi - p(\operatorname{div}(\psi)) \, \mathrm{d}x = \int_D f \cdot \psi \, \mathrm{d}x, \text{ for all } \psi \in V.$$

Now multiplying the second equation with $\varphi \in H$ and integrating, one can formulate the following variational formulation of the problem:

Variational formulation for the Stokes equation with no-slip boundary condition

Seek $v \in V$ and $p \in H$ such that

$$\int_D \nabla v \cdot \nabla \psi - p(\operatorname{div}(\psi)) \, \mathrm{d}x = \int_D f \cdot \psi \, \mathrm{d}x, \text{ for all } \psi \in V, \text{ and}$$

$$\int_D \varphi(\operatorname{div}(v)) \, \mathrm{d}x = 0, \text{ for all } \varphi \in H.$$

To use the finite element method, one needs to find a discrete analogue of the variational formulation. It is possible, but there are some issues when choosing the

finite dimensional subspaces V_h and H_h. These issues, concerning for example the stability of the solution, will not be explained here, but a discussion can be found in Johnson [3, pp. 232ff]. One observation of importance for the solution and the attached MATLAB code, though, is that one has to have $\dim(V_h) \geq \dim(H_h)$ ([3, p. 237]).

The natural approach is to let $V_h = U_h \times U_h$, where a basis for U_h is the usual piecewise linear functions where $\psi_i \in U_h$ equal one on the interior node i and zero on all other nodes (see Figure 3.3). A basis for V_h is then

$$\left\{ \begin{bmatrix} \psi_1 \\ 0 \end{bmatrix}, ..., \begin{bmatrix} \psi_N \\ 0 \end{bmatrix}, \begin{bmatrix} 0 \\ \psi_1 \end{bmatrix}, ..., \begin{bmatrix} 0 \\ \psi_N \end{bmatrix} \right\},$$

where $N = \dim(U_h)$, and a basis for H_h are the locally constant functions where $\varphi_j \in H_h$ equal one on triangle j and zero else, where we let $M = \dim(H_h)$.[2]

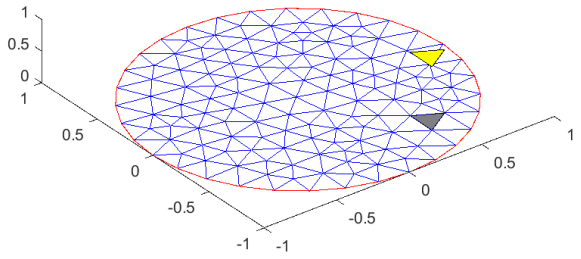

Figure 4.5: An example of a basis function $\varphi \in H_h$. Note that it equals one on the marked triangle, but zero everywhere else.

To be able to use these spaces and at the same time fulfill the condition $\dim(V_h) = 2N \geq \dim(H_h) = M$, two different meshes need to be used to produce the solutions in this section. The mesh used to define V_h was created by refining the mesh defining H_h, such that each node in the mesh defining H_h is also a node in the finer mesh. This is illustrated in the pictures below.

[2]The reason this is a natural choice, leading to the use of different basis functions for U_h and H_h, is that by the variational formulation we need to assume that the first derivatives of v belongs to $L_2(D)$, since for example ∇v appears in the equations, while this is not the case for the pressure p.

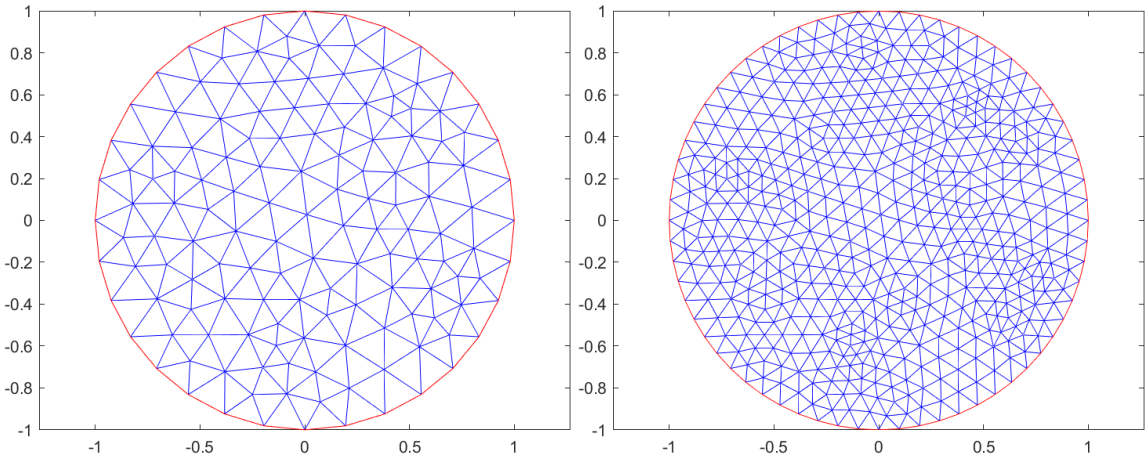

Figure 4.6: Possible meshes for defining H_h respectively V_h.

The finite element method for the Stokes problem with no-slip boundary condition now reads:

FEM for the Stokes equation with no-slip boundary condition

Seek $v_h \in V_h$ and $p_h \in H_h$ such that

$$\int_D \nabla v_h \cdot \nabla v - p_h(\operatorname{div}(v))\,\mathrm{d}x = \int_D f \cdot v\,\mathrm{d}x, \text{ for all } v \in V_h, \text{ and}$$

$$\int_D p(\operatorname{div}(v_h))\,\mathrm{d}x = 0, \text{ for all } p \in H_h.$$

Letting $v = \sum_{i=1}^{2N} \xi_i \psi_i$ and $p = \sum_{i=1}^{M} \eta_i \varphi_i$, this can be written in matrix form as

$$\begin{cases} A\boldsymbol{\xi} - B\boldsymbol{\eta} = F \\ B^T\boldsymbol{\xi} = 0, \end{cases}$$

where

$$A = (a_{ij}) \text{ with } a_{ij} = \int_D \nabla\psi_i \cdot \nabla\psi_j\,\mathrm{d}x,\ 1 \le i, j \le 2N,$$

$$B = (b_{ij}) \text{ with } b_{ij} = \int_D \varphi_j(\operatorname{div}(\psi_i))\,\mathrm{d}x,\ 1 \le i \le 2N,\ 1 \le j \le M, \text{ and}$$

$$F = (f_j) \text{ with } f_j = \int_D f \cdot \psi_j\,\mathrm{d}x,\ 1 \le j \le M.$$

This can be solved as one large system of equations by assembling a block $(2N + M) \times (2N + M)-$matrix $\boldsymbol{M}$ as

$$\boldsymbol{M} = \begin{bmatrix} A_1 & 0 & -B_1 \\ 0 & A_2 & -B_2 \\ B_1^T & B_2^T & 0 \end{bmatrix},$$

where

$$A_1 = (a_{1_{ij}}), \text{ with } (a_{1_{ij}}) = \int_D \nabla\psi_i \cdot \nabla\psi_j \, \mathrm{d}x \text{ for } 1 \leq i, j \leq N,$$

$$A_2 = (a_{2_{i-N,j-N}}), \text{ with } (a_{2_{i-N,j-N}}) = \int_D \nabla\psi_i \cdot \nabla\psi_j \, \mathrm{d}x \text{ for } N+1 \leq i, j \leq 2N,$$

$$B_1 = (b_{1_{ij}}), \text{ with } (b_{1_{ij}}) = \int_D \varphi_j(\mathrm{div}(\psi_i)) \, \mathrm{d}x \text{ for } 1 \leq i \leq N \text{ and } 1 \leq j \leq M, \text{ and}$$

$$B_2 = (b_{2_{i-N,j}}), \text{ with } (b_{2_{i-N,j}}) = \int_D \varphi_j(\mathrm{div}(\psi_i)) \, \mathrm{d}x \text{ for } N+1 \leq i \leq 2N \text{ and } 1 \leq j \leq M.$$

Letting $\boldsymbol{\xi_1} = \begin{bmatrix} \xi_1 & \xi_2 & ... & \xi_N \end{bmatrix}^T$, $\boldsymbol{\xi_2} = \begin{bmatrix} \xi_{N+1} & \xi_{N+2} & ... & \xi_{2N} \end{bmatrix}^T$, $\boldsymbol{\eta} = \begin{bmatrix} \eta_1 & \eta_2 & ... & \eta_M \end{bmatrix}^T$, $F_1 = \begin{bmatrix} f_1 & f_2 & ... & f_N \end{bmatrix}^T$ and $F_2 = \begin{bmatrix} f_{N+1} & f_{N+2} & ... & f_{2N} \end{bmatrix}^T$, the equation system to be solved is

$$\begin{bmatrix} A_1 & 0 & -B_1 \\ 0 & A_2 & -B_2 \\ B_1^T & B_2^T & 0 \end{bmatrix} \begin{bmatrix} \boldsymbol{\xi_1} \\ \boldsymbol{\xi_2} \\ \boldsymbol{\eta} \end{bmatrix} = \begin{bmatrix} F_1 \\ F_2 \\ 0 \end{bmatrix}.$$

Below are plots of the solution to the Stokes equation with the no-slip boundary condition, with the same input f as in the previous section, Figure 4.1.

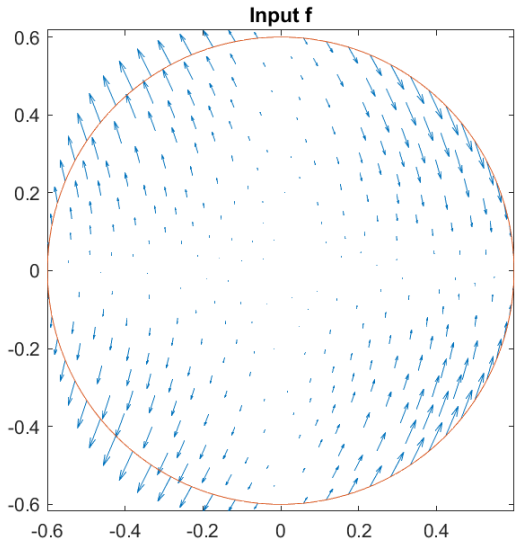

(a) The external force f.

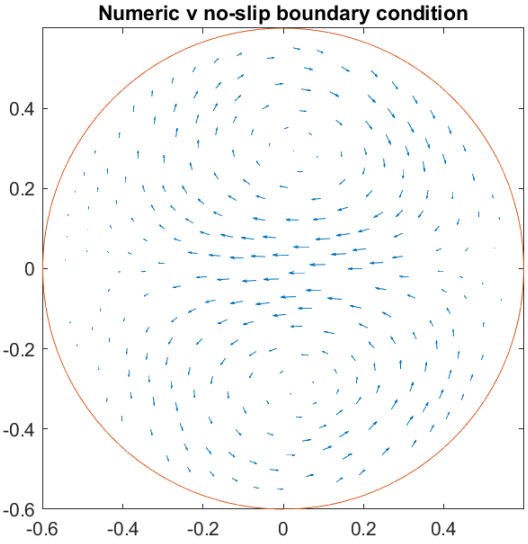

(b) The velocity field v.

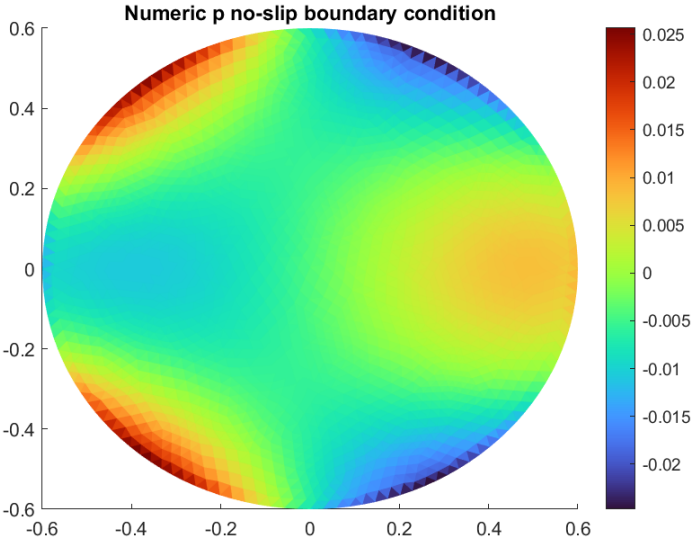

(c) The pressure p.

Figure 4.7: Solution to the Stokes equation with no-slip boundary condition (4.4). As in Section 4.2, the field $f = xy^2e_1 - xye_2$ is plotted with the in-built autoscale function of the MATLAB command 'quiver' but the vector field v is scaled with the factor 50.

The directions of the vectors in v seem to in large match the solution with Hodge boundary conditions, but there are some differences. As can be seen in the pictures, the velocity field v is zero at the boundary, contrary to the case with Hodge boundary conditions in Figure 4.1. This leads to the most striking difference in the pressure, to the right in the plot d). With Hodge boundary conditions, allowing the flow to slip at the boundary, the velocity field "points" at this region both from above and below, causing the pressure to rise higher than in the case of the no-slip boundary condition, where the velocity at the boundary is zero and thereby the flow into the

region is smaller. Another big difference is that the velocity overall is smaller in the solution with the no-slip boundary condition. It seems like the fact that the viscous flow sticks at the boundary slows down the flow in the whole domain. One should also mention that for the technical reasons discussed earlier in this section, the plots for the velocity field and the pressure in this section have been made from two different meshes with the pressure plot made from triangular data instead of nodal data. The finer mesh in this section, used for the velocity field, is the same as the one used to produce the plots in section 4.2.

CHAPTER 5

Discussion and conclusions

The main goal of this thesis is to show results from a project about investigating and analysing the solution of the Stokes equation under the Hodge boundary conditions. Referring to the solutions in Sections 4.2 and 4.3 of this thesis, it is not hard to argue that the Hodge boundary conditions are more mathematically natural than the no-slip boundary condition. With the Hodge boundary conditions, one can solve the problem step by step using the tangential Hodge decomposition theorem (3.1.6) with Corollary 3.3.1 to guarantee the uniqueness in every step. To begin with, the boundary condition $\hat{n} \lrcorner \omega = 0$ on ∂D, which in two dimension translates to $\omega|_{\partial D} = 0$, makes sure that $\delta\omega \in R(\underline{\delta})$, and since ∇p clearly belongs to $R(d)$, the Hodge decomposition theorem is applicable to find $\delta\omega$ and dp. In the following parts of the solution, one can then proceed to use the subspaces $R(d)$ and $R(\underline{\delta})$ from the tangential Hodge decomposition and Corollary 3.3.1 to get the desired uniqueness results. The application of the theory is thus very smooth. When using the no-slip boundary condition, the solution can not follow the same pattern, since the boundary condition $v|_{\partial D} = 0$ does not translate as well into the theory of Hodge decompositions.

The Hodge boundary conditions also provide the possibility of a simpler solution from a numerical perspective. By applying the tangential Hodge decomposition theorem, the problem in Section 4.2 can thereafter be solved with the finite element method applied to quite simple partial differential equations. The solution in Section 4.3 with the no-slip boundary condition on the other hand requires a mixed finite element method, using two different test spaces. An additional requirement concerns the dimension of the test spaces, for the problem in this thesis leading to the need of two different meshes to be able to compute a solution. Apart from this there are, as mentioned briefly in Section 4.3, some issues concerning for example the stability of the solution. These issues are beyond the scope of this thesis, but the following citation from Johnson [3, p. 233] gives a hint about these problems:

> *(...) the spaces V_h and H_h will have to be conveniently chosen; not just any combination will work. Loosely speaking, we want to choose V_h and H_h so that the resulting method is both stable and accurate. These demands are in some sense conflicting and one has to find a reasonable compromise (...)*

It should, though, be mentioned that the above citation is about the solution of the Stokes equation specifically with the finite element method. There may be other, better suited, methods for finding numerical solutions that has not been mentioned in this thesis.

Although the Hodge boundary conditions provide a mathematically smooth way of solving the Stokes equation, they do not model physical flows. They are contrary to the known fact that viscous flows stick to the boundary. In Section 4.2 of this thesis it is shown that the Hodge boundary conditions can be interpreted as a situation where the friction at the boundary only depends on the geometry of the domain, or to be precise: the curvature of the boundary. At a non-convex part of the boundary, as in Figure 4.2c) and d), the friction is negative, which is not possible from a physical point of view. Another problem for the algorithm presented in Section 4.2 is the demand that the external forces f should be orthogonal to $C_{\shortparallel}(D)$. For a simply connected domain D this is not a problem since $C_{\shortparallel}(D; \wedge^1) = \{0\}$, but if the domain is not simply connected it may cause problems in some cases. The pictures below shows an example.

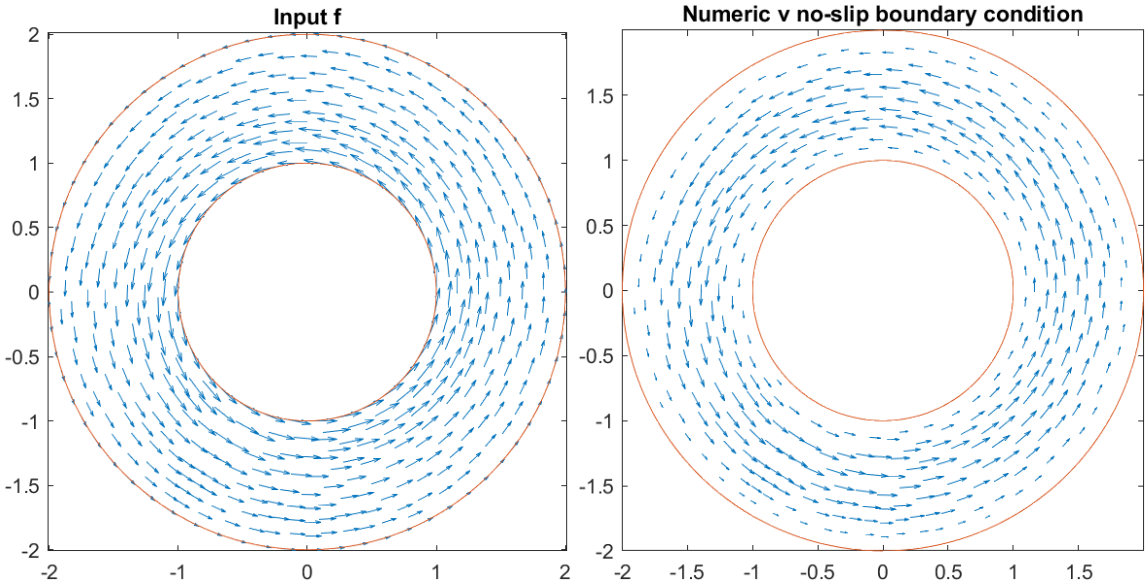

(a) The external force $f = \frac{-ye_1}{x^2+y^2} + \frac{xe_2}{x^2+y^2}$, plotted with autoscale.

(b) v computed with the no-slip boundary condition, 2:1-scale.

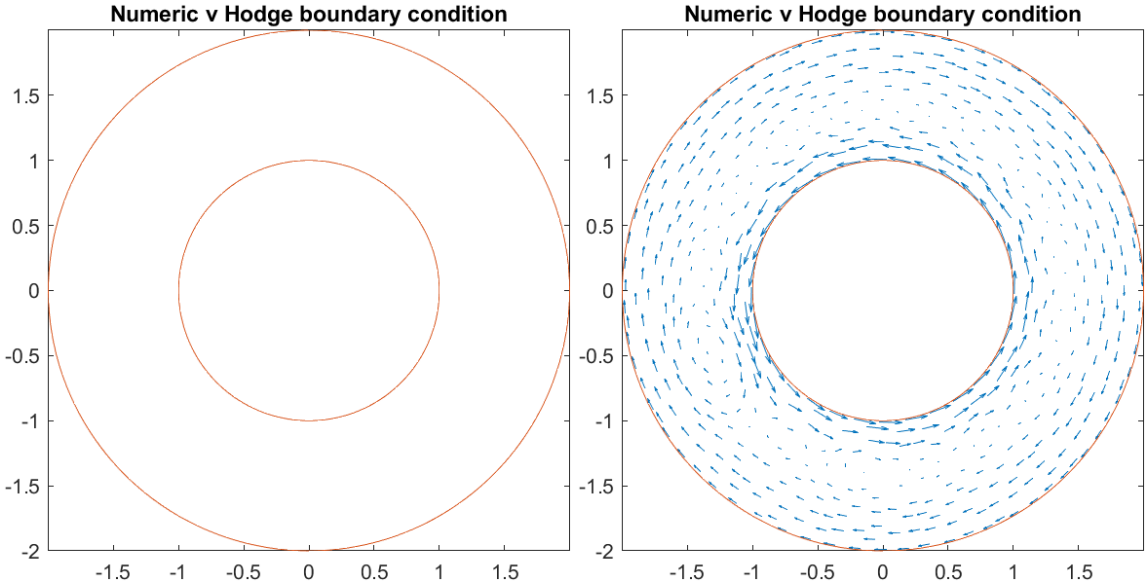

(c) v, computed with the Hodge boundary conditions, 2:1-scale.

(d) v, computed with the Hodge boundary conditions, plotted with autoscale.

Figure 5.1: The velocity field v in the Stokes equation under different boundary conditions, when trying to impose the algorithms described in Sections 4.2 and 4.3 with an external force field $f \in C_{||}(D)$.

As can be seen in Figure 5.1, the results when imposing the algorithms from Sections 4.2 and 4.3 are very different. Since $f \in C_{||}(D)$, the Hodge decomposition in the beginning of the algorithm of Section 4.2 gives $p = \omega = dv = 0$ (modulo computational errors), and the resulting velocity field is zero. The velocity field from the Hodge boundary conditions plotted with autoscale, Figure 5.1d), enforces the feeling that

the result does not make sense. Using the no-slip boundary condition, though, gives a result shown in Figure 5.1b) which corresponds well with the physical intuition.

A secondary goal of this thesis is to show a glimpse of how the different concepts of derivative in vector calculus fit well into the framework of multivector analysis. While vector calculus often restricts to two or three dimensions, defining for example the *curl* of a vector field F in three dimensions as $\nabla \times F$, the multivector analysis provides generalisations of the concepts gradient, divergence, and curl, working in arbitrary dimensions. In this thesis, attention has been restricted to Euclidean spaces and mostly to simply-connected domains in $\mathbb{R}^2$, but the multivector analysis covers a lot more than this.

In summary, this thesis may provide a brief introduction to multivector analysis and a small contribution to the understanding of the Hodge boundary conditions for the Stokes equation. A natural next step would be to extend the study of the Hodge boundary conditions to cases with a three-dimensional domain.

CHAPTER A

Appendix: MATLAB code

In this chapter the MATLAB code written for this project is attached. The code is, unless mentioned otherwise, written in full by the author.

A.1 Main programs

In this section the code for the main programs is presented. The pdeModeler application has been used to create triangulations. The variables p, e, t, and g come from these triangulations, where p is the default name for the matrix containing the coordinates of the nodes in the mesh, e is a matrix containing (among others) coordinates for the nodes on the boundary, t is a matrix containing the triangles, and g is used to plot the boundary of the domain. In the code for the solution of the Stokes equation with no-slip boundary condition, two meshes are used. The triple (p, e, t) constitutes the mesh used for the pressure function and (p2, e2, t2) the finer mesh used for the velocity field (see Section 4.3).

Tangential Hodge decomposition

```
N = size(p, 2);
A = zeros(N, N);
b = zeros(N, 1);
F1 = @(x, y) 2*y*(1-x^2-y^2) + y-3*x^2*y^3; %The vector
   field in Figure 3.1
F2 = @(x, y) -2*x*(1-x^2-y^2) + x-3*x^3*y; %The vector
   field in Figure 3.1
%F1 = @(x, y) -2*x*(1-x^2-y^2)+4*x*y^2 + 2*x*y-3*x^2*y^2;
    %The vector field in Figure 3.4
%F2 = @(x, y) 2*y*(1-x^2-y^2)-4*x^2*y + x^2-2*x^3*y; %The
    vector field in Figure 3.4
starF2 = @ (x, y) -F1(x, y);
for el = 1 : size(t, 2)
    nn = t(1:3, el);
    A(nn, nn) = A(nn, nn) + IntMatrix(p(:, nn));
    b(nn) = b(nn) + IntVector(F1, F2, p(:, nn));
end
```

```
ux = A\b; %Coefficients for U
N2 = size(p, 2);
A2 = zeros(N2, N2);
b2 = zeros(N2, 1);
for el = 1 : size(t, 2)
    nn = t(1:3, el);
    A2(nn, nn) = A2(nn, nn) + IntMatrix(p(:, nn));
    b2(nn) = b2(nn) + IntVector(F2, starF2, p(:, nn));
end
intnodes = setdiff(1:N2, e(1, :)); %Used to impose the
   homogeneous Dirichlet bc
ADir = A2(intnodes, intnodes);
bDir = b2(intnodes);
xDir = ADir\bDir;
ux2 = zeros(N2, 1);
ux2(intnodes) = xDir; %Coefficients for V
gradmatrixu = twodimgradmatrix(p, t, ux);
rotmatrixv = twodimgradmatrixv(p, t, ux2);
X = [];
Y = [];
for s = 1:numel(t(1, :)) %Find middle of triangles in
   mesh
    Xmiddle = (p(1, t(1,s)) + p(1, t(2,s)) + p(1, t(3,s))
       )/3;
    Ymiddle = (p(2, t(1,s)) + p(2, t(2,s)) + p(2, t(3,s))
       )/3;
    X = [X, Xmiddle];
    Y = [Y, Ymiddle];
end
cohmatrixh = [];
for hx = 1:numel(X) %Compute cohomology field
    cohmatrixh(1,hx) = F1(X(hx), Y(hx))-gradmatrixu(1, hx
       )-rotmatrixv(1, hx);
    cohmatrixh(2,hx) = F2(X(hx), Y(hx))-gradmatrixu(2, hx
       )-rotmatrixv(2, hx);
end
vectorfieldmatrix = []; %Computing the values for the
   input f
for vf = 1:numel(X)
    vectorfieldmatrix(1, vf) = F1(X(vf), Y(vf));
    vectorfieldmatrix(2, vf) = F2(X(vf), Y(vf));
end
for rd = 1:numel(X)-1 %The code below reduces the plots
    Xtest = X(rd);
    Ytest = Y(rd);
    for rc = rd+1:numel(X)
```

```
        if sqrt((X(rc)-Xtest)^2+(Y(rc)-Ytest)^2) < 0.05
            X(rc) = 99;
            Y(rc) = 99;
            vectorfieldmatrix(:, rc) = 99;
            gradmatrixu(:, rc) = 99;
            rotmatrixv(:, rc) = 99;
            cohmatrixh(:, rc) = 99;
        end
    end
end
for rv = numel(X):-1:1
    if X(rv) == 99
        X(rv) = [];
    end
    if Y(rv) == 99
        Y(rv) = [];
    end
    if vectorfieldmatrix(1, rv) == 99 & vectorfieldmatrix
       (2, rv) == 99
        vectorfieldmatrix(:, rv) = [];
    end
    if gradmatrixu(1, rv) == 99 & gradmatrixu(2, rv) ==
       99
        gradmatrixu(:, rv) = [];
    end
    if rotmatrixv(1, rv) == 99 & rotmatrixv(2, rv) == 99
        rotmatrixv(:, rv) = [];
    end
    if cohmatrixh(1, rv) == 99 & cohmatrixh(2, rv) == 99
        cohmatrixh(:, rv) = [];
    end
end %Last line of the plot reducing
scalefactor = 0.075; %Used to make the vector field plots
    in the same scale
figure(1) %Plots input f
quiver(X, Y, vectorfieldmatrix(1, :)*scalefactor,
   vectorfieldmatrix(2, :)*scalefactor, 0);
hold on
pdegplot(g);
figure(2) %Plots \nabla U
quiver(X, Y, gradmatrixu(1, :)*scalefactor, gradmatrixu
   (2, :)*scalefactor, 0);
hold on
pdegplot(g);
figure(3) %Plots \nabla \lrcorner V
```

```
quiver(X, Y, rotmatrixv(1, :)*scalefactor, rotmatrixv(2,
   :)*scalefactor, 0);
hold on
pdegplot(g);
figure(4) %Plots the cohomology field
quiver(X, Y, cohmatrixh(1, :)*scalefactor, cohmatrixh(2,
   :)*scalefactor, 0);
hold on
pdegplot(g);
hold on
```

The Stokes equation with Hodge boundary conditions

```
F1 = @(x, y) x*y^2; %Input f in Chapter 4
F2 = @(x, y) -x*y; %Input f in Chapter 4
%F1 = @(x, y) -y/(x^2 + y^2); %Input f in Chapter 5
%F2 = @(x, y) x/(x^2 + y^2); %Input f in Chapter 5
starF2 = @(x, y) -F1(x, y);
visc = -1; %Viscousity=1
N2 = size(p, 2);
A2 = zeros(N2, N2);
b3 = zeros(N2, 1);
b2 = zeros(N2, 1);
b = zeros(N2, 1);
for el = 1 : size(t, 2)
    nn = t(1:3, el);
    A2(nn, nn) = A2(nn, nn) + IntMatrix(p(:, nn));
    b3(nn) = b3(nn) + IntVector(F1, F2, p(:, nn));
end
pressure = A2\b3; %Coefficients for p
gradmatrixp = twodimgradmatrix(p, t, pressure);
for el = 1 : size(t, 2)
    nn = t(1:3, el);
    b2(nn) = b2(nn) + IntVector(F2, starF2, p(:, nn));
end
intnodes = setdiff(1:N2, e(1, :));
ADir = A2(intnodes, intnodes);
bDir = b2(intnodes);
xDir = ADir\bDir;
ux2 = zeros(N2, 1);
ux2(intnodes) = xDir/visc; %Coefficients for omega
starw = scatteredInterpolant(p(1, :)', p(2, :)', ux2);
for elm = 1 : size(t, 2)
    nn = t(1:3, elm);
    b(nn) = b(nn) + IntVectorDN(starw, p(:, nn));
end
```

```
bDirproblem = b(intnodes);
xDirproblem = ADir\bDirproblem;
ux = zeros(N2, 1);
ux(intnodes) = xDirproblem; %Phi
gradux = twodimgradmatrix(p, t, ux);
graduxstar = [-gradux(2, :); gradux(1, :)]; %The velocity
    field v
X = [];
Y = [];
for s = 1:numel(t(1, :)) %Find middle of triangles in
   mesh
    Xmiddle = (p(1, t(1,s)) + p(1, t(2,s)) + p(1, t(3,s))
       )/3;
    Ymiddle = (p(2, t(1,s)) + p(2, t(2,s)) + p(2, t(3,s))
       )/3;
    X = [X, Xmiddle];
    Y = [Y, Ymiddle];
end
for rd = 1:numel(X)-1 %Reducing plot.
    Xtest = X(rd);
    Ytest = Y(rd);
    for rc = rd+1:numel(X)
        if sqrt((X(rc)-Xtest)^2+(Y(rc)-Ytest)^2) < 0.1
            X(rc) = 99;
            Y(rc) = 99;
            graduxstar(:, rc) = 99;
            gradmatrixp(:, rc) = 99;
        end
    end
end
for rv = numel(X):-1:1
    if X(rv) == 99
        X(rv) = [];
    end
    if Y(rv) == 99
        Y(rv) = [];
    end
    if graduxstar(1, rv) == 99 && graduxstar(2, rv) == 99
        graduxstar(:, rv) = [];
    end
    if gradmatrixp(1, rv) == 99 && gradmatrixp(2, rv) ==
       99
        gradmatrixp(:, rv) = [];
    end
end
inputf = [];
```

```
for xs = 1:numel(X)
    inputf(1,xs) = F1(X(xs), Y(xs));
    inputf(2,xs) = F2(X(xs), Y(xs));
end
scalefactor = 1;
figure(1) %Plots v
quiver(X, Y, scalefactor*graduxstar(1, :), scalefactor*
   graduxstar(2, :), 0);
hold on
pdegplot(g);
title('Numeric v Hodge boundary condition')
figure(2) %Plots p
pdesurf(p, t, pressure)
colormap turbo
title('Numeric p Hodge boundary condition')
figure(3) %Plots input f
quiver(X, Y, inputf(1, :), inputf(2, :));
hold on
pdegplot(g)
title('Input f')
```

The Stokes equation with no-slip boundary condition

```
F1 = @(x, y) x*y^2; %Input f in Chapter 4
F2 = @(x, y) -x*y; %Input f in Chapter 4
%F1 = @(x, y) -y/(x^2 + y^2); %Input f in Chapter 5
%F2 = @(x, y) x/(x^2 + y^2); %Input f in Chapter 5
N = size(p2, 2);
M = size(t, 2);
A = zeros(N, N);
b3 = zeros(M, 1);
b2 = zeros(N, 1);
b = zeros(N, 1);
preFillingN = zeros(N, N);
FillingM = zeros(M, M);
for el = 1 : size(t2, 2)
    nn = t2(1:3, el);
    A(nn, nn) = A(nn, nn) + IntMatrix(p2(:, nn));
    b(nn) = b(nn) + IntVectorDN(F1, p2(:, nn));
    b2(nn) = b2(nn) + IntVectorDN(F2, p2(:, nn));
end
Bx = Bmatrixdx3(t, t2, p, p2); %Putting together matrices
    for the big block matrix M
By = Bmatrixdy3(t, t2, p, p2);
intnodes = setdiff(1:N, e2(1, :));
FillingN = preFillingN(intnodes, intnodes);
```

```
AF = A(intnodes, intnodes);
BxF = Bx(intnodes, :);
ByF = By(intnodes, :);
BxFt = transpose(BxF);
ByFt = transpose(ByF);
bF = b(intnodes);
b2F = b2(intnodes);
FinalMatrix = [AF FillingN -BxF; FillingN AF -ByF; BxFt
   ByFt FillingM]; %The block matrix M
FinalVector = -[bF; b2F; b3]; %(Minus because of
   construction of IntVectorDN)
Finalanswer = FinalMatrix\FinalVector; %The answer with
   coefficients for v1, v2 and p
v1numeric = zeros(N, 1);
v2numeric = zeros(N, 1);
v1numeric(intnodes) = Finalanswer(1:numel(intnodes));
v2numeric(intnodes) = Finalanswer(numel(intnodes)+1:2*
   numel(intnodes));
pnumeric = Finalanswer(2*numel(intnodes)+1:end);
f1input = [];
f2input = [];
for na = 1:numel(p2(1, :))
    f1input(na) = F1(p2(1, na), p2(2, na));
    f2input(na) = F2(p2(1, na), p2(2, na));
end
X = [];
Y = [];
for s = 1:numel(t(1, :)) %Find middle of triangles in
   mesh
    Xmiddle = (p(1, t(1,s)) + p(1, t(2,s)) + p(1, t(3,s))
       )/3;
    Ymiddle = (p(2, t(1,s)) + p(2, t(2,s)) + p(2, t(3,s))
       )/3;
    X = [X, Xmiddle];
    Y = [Y, Ymiddle];
end
XN = p2(1, :);
YN = p2(2, :);
for rn = 1:numel(XN)-1 %Reduce plot
    XNtest = XN(rn);
    YNtest = YN(rn);
    for rcn = rn+1:numel(XN)
        if sqrt((XN(rcn)-XNtest)^2+(YN(rcn)-YNtest)^2) <
           0.05
            XN(rcn) = 99;
            YN(rcn) = 99;
```

```
            f1input(rcn) = 99;
            f2input(rcn) = 99;
            v1numeric(rcn) = 99;
            v2numeric(rcn) = 99;
        end
    end
end
for rnv = numel(XN):-1:1
    if XN(rnv) == 99
        XN(rnv) = [];
    end
    if YN(rnv) == 99
        YN(rnv) = [];
    end
    if f1input(rnv) == 99 && f2input(rnv) == 99
        f1input(rnv) = [];
        f2input(rnv) = [];
    end
    if v1numeric(rnv) == 99 && v2numeric(rnv) == 99
        v1numeric(rnv) = [];
        v2numeric(rnv) = [];
    end
end
scalefactor = 2;
figure(1) %Plots input f
quiver(XN', YN', f1input', f2input');
hold on
pdegplot(g)
title('Input f')
figure(2) %Plots v
quiver(XN, YN, scalefactor*v1numeric', scalefactor*
   v2numeric', 0);
hold on
pdegplot(g)
title('Numeric v no-slip boundary condition')
figure(3) %Plots p
pdesurf(p, t, pnumeric')
colormap turbo
title('Numeric p no-slip boundary condition')
```

Vector lengths

This code starts with a tangential Hodge decomposition above, then the below code is added before reducing the plot. The input used in Figure 4.2 is $f = (x+y)e_1 + (x^2 - y^2)e_2$.

```
vectorlengthsv = [];
for vx = 1:numel(graduxstar(1, :))
    vectorlengthsv(vx) = sqrt(graduxstar(1, vx)^2 +
       graduxstar(2, vx)^2);
end
figure(1) %Used for the 2d-plots
pdesurf(p, t, vectorlengthsv)
colormap('turbo')
xlim([-1 1])
ylim([-1 1])
ut = pdeprtni(p, t, vectorlengthsv);
figure(2) %Used for the 3d-plots
pdesurf(p, t, ut)
colormap('turbo')
```

A.2 Functions

In this section code of the functions used in the main programs is presented.

IntMatrix

Computes the matrix $\int_D \nabla\psi_i \cdot \nabla\psi_j \, \mathrm{d}x$. The code for this function is taken from [7, p. 191].

```
function A0 = IntMatrix(nodes)
%Input: 2x3 matrix, node coordinates as columns
%Output 3x3 matrix of integrals for stiffness matrix
e1 = nodes(:, 1) - nodes(:, 3); %choose 3rd node as
   origin
e2 = nodes(:, 2) - nodes(:, 3);
basis = [e1, e2];
dualbasis = inv(basis'); %Computes the dual basis
grads = [dualbasis(:, 1), dualbasis(:, 2), -dualbasis(:,
   1) - dualbasis(:, 2)];
area = det(basis)/2; %Computes the area of the triangle
A0 = grads' * grads * area; %Returns the 9 inner products
end
```

IntVector

Computes the load vector $\int_D f\psi_i dx$.

```
function B0 = IntVector(F1, F2, nodes)
%F vector field
```

```
%nodes as in IntMatrix
%output 3x1 matrix
B0 = zeros(3,1);
e1 = nodes(:, 1) - nodes(:, 3); %choose 3rd node as
   origin
e2 = nodes(:, 2) - nodes(:, 3);
basis = [e1, e2];
dualbasis = inv(basis'); %computes the dual basis
grads = [dualbasis(:, 1), dualbasis(:, 2), -dualbasis(:,
   1) - dualbasis(:, 2)];
area = det(basis)/2;
for m = 1:3
    B0(m) = (1/3)*area*(grads(1,m)*(F1((nodes(1,1)+nodes
       (1,2))/2, (nodes(2,1)+nodes(2,2))/2) + F1((nodes
       (1,2)+nodes(1,3))/2, (nodes(2,2)+nodes(2,3))/2) +
       F1((nodes(1,3)+nodes(1,1))/2, (nodes(2,3)+nodes
       (2,1))/2)) + grads(2,m)*(F2((nodes(1,1)+nodes(1,2))
       /2, (nodes(2,1)+nodes(2,2))/2) + F2((nodes(1,2)+
       nodes(1,3))/2, (nodes(2,2)+nodes(2,3))/2) + F2((
       nodes(1,3)+nodes(1,1))/2, (nodes(2,3)+nodes(2,1))
       /2)));
end
```

twodimgradmatrix

Computes $\nabla \wedge U$ in the tangential Hodge decomposition.

```
function gradmatrix = twodimgradmatrix(p, t, u)
Fx = [];
Fy = [];
for n = 1:numel(t(1, :))
    p1 = p(:, t(1, n)); %Find coordinates for nodes
    p2 = p(:, t(2, n));
    p3 = p(:, t(3, n));
    v1 = [p2(1)-p1(1), p2(2)-p1(2), u(t(2, n))-u(t(1, n))
       ]; %Create vectors for finding plane
    v2 = [p3(1)-p1(1), p3(2)-p1(2), u(t(3, n))-u(t(1, n))
       ];
    V = cross(v1, v2); %Normal vector for plane
    Fx = [Fx, V(1)/(-V(3))];
    Fy = [Fy, V(2)/(-V(3))];
end
gradmatrix = [Fx; Fy];
```

twodimgradmatrixv

Computes $\nabla \lrcorner V$ in the tangential Hodge decomposition.

```
function gradmatrix = twodimgradmatrixv(p, t, u)
Fx = [];
Fy = [];
for n = 1:numel(t(1, :))
    p1 = p(:, t(1, n)); %Find coordinates for nodes
    p2 = p(:, t(2, n));
    p3 = p(:, t(3, n));
    v1 = [p2(1)-p1(1), p2(2)-p1(2), u(t(2, n))-u(t(1, n))
       ]; %Create vectors for finding plane
    v2 = [p3(1)-p1(1), p3(2)-p1(2), u(t(3, n))-u(t(1, n))
       ];
    V = cross(v1, v2); %Normal vector for plane
    Fx = [Fx, -1*(V(2)/(-V(3)))];
    Fy = [Fy, (V(1)/(-V(3)))];
end
gradmatrix = [Fx; Fy];
```

IntVectorDN

Computes the load vector in the Dirichlet (or Neumann) problem.

```
function B0dn = IntVectorDN(F, nodes)
%F vector field
%nodes as in IntMatrix
%output 3x1 matrix
B0dn = zeros(3,1);
e1 = nodes(:, 1) - nodes(:, 3); %choose 3rd node as
   origin
e2 = nodes(:, 2) - nodes(:, 3);
basis = [e1, e2];
area = det(basis)/2;
for m = 1:3
    coeffmatrix = [nodes(1, mod(m, 3)+1), nodes(2, mod(m,
        3)+1), 1; nodes(1, mod(m+1, 3)+1), nodes(2, mod(m
       +1, 3)+1), 1; nodes(1, mod(m+2, 3)+1), nodes(2,
       mod(m+2, 3)+1), 1];
    solvector = [1; 0; 0];
    phicoeffs = coeffmatrix\solvector;
    phi = @ (x, y) (phicoeffs(1)*x+phicoeffs(2)*y+
       phicoeffs(3)).*F(x, y);
    B0dn(mod(m,3)+1) = -1 * 1/3 * area * (phi((nodes(1,1)
       +nodes(1,2))/2, (nodes(2,1)+nodes(2,2))/2) + phi((
```

```
        nodes(1,2)+nodes(1,3))/2, (nodes(2,2)+nodes(2,3))
        /2) + phi((nodes(1,1)+nodes(1,3))/2, (nodes(2,1)+
        nodes(2,3))/2));
end
```

Bmatrixdx3

Computes the matrix B_1 in the big block matrix M from Section 4.3.

```
function Bx = Bmatrixdx3(t, t2, p, p2) %t, p = mesh for
   Pressure, t2, p2 = mesh for v
Bx = zeros(numel(t2(1, :)), numel(t(1, :)));
for bt = 1:numel(t(1, :))
    A = t(1, bt); %Vertices for pressure triangle
    B = t(2, bt);
    C = t(3, bt);
    bigtrianglex = [p(1, A) p(1, B) p(1, C) p(1, A)];
    bigtriangley = [p(2, A) p(2, B) p(2, C) p(2, A)];
    for st = 1:numel(t2(1, :))
        a = t2(1, st); %Vertices for small triangle
        b = t2(2, st);
        c = t2(3, st);
        if inpolygon(p2(1, a), p2(2, a), bigtrianglex,
           bigtriangley) && inpolygon(p2(1, b), p2(2, b),
            bigtrianglex, bigtriangley) && inpolygon(p2
           (1, c), p2(2, c), bigtrianglex, bigtriangley)
            coefficientmatrix = [p2(1, a) p2(2, a) 1; p2
               (1, b) p2(2, b) 1; p2(1, c) p2(2, c) 1];
            e1 = p2(:, a) - p2(:, c);
            e2 = p2(:, b) - p2(:, c);
            basis = [e1, e2];
            area = det(basis)/2;
            ahat = coefficientmatrix\[1 0 0]';
            bhat = coefficientmatrix\[0 1 0]';
            chat = coefficientmatrix\[0 0 1]';
            Bx(a, bt) = Bx(a, bt) + area*ahat(1);
            Bx(b, bt) = Bx(b, bt) + area*bhat(1);
            Bx(c, bt) = Bx(c, bt) + area*chat(1);
        end
    end
end
```

Bmatrixdy3

Computes the matrix B_2 in the big block matrix M from Section 4.3.

```
function By = Bmatrixdy3(t, t2, p, p2) %t, p = mesh for
   Pressure, t2, p2 = mesh for v
By = zeros(numel(t2(1, :)), numel(t(1, :)));
for bt = 1:numel(t(1, :))
    A = t(1, bt); %Vertices for pressure triangle
    B = t(2, bt);
    C = t(3, bt);
    bigtrianglex = [p(1, A) p(1, B) p(1, C) p(1, A)];
    bigtriangley = [p(2, A) p(2, B) p(2, C) p(2, A)];
    for st = 1:numel(t2(1, :))
        a = t2(1, st); %Vertices for small triangle
        b = t2(2, st);
        c = t2(3, st);
        if inpolygon(p2(1, a), p2(2, a), bigtrianglex,
           bigtriangley) && inpolygon(p2(1, b), p2(2, b),
            bigtrianglex, bigtriangley) && inpolygon(p2
           (1, c), p2(2, c), bigtrianglex, bigtriangley)
            coefficientmatrix = [p2(1, a) p2(2, a) 1; p2
               (1, b) p2(2, b) 1; p2(1, c) p2(2, c) 1];
            e1 = p2(:, a) - p2(:, c);
            e2 = p2(:, b) - p2(:, c);
            basis = [e1, e2];
            area = det(basis)/2;
            ahat = coefficientmatrix\[1 0 0]';
            bhat = coefficientmatrix\[0 1 0]';
            chat = coefficientmatrix\[0 0 1]';
            By(a, bt) = By(a, bt) + area*ahat(2);
            By(b, bt) = By(b, bt) + area*bhat(2);
            By(c, bt) = By(c, bt) + area*chat(2);
        end
    end
end
```

Bibliography

[1] Asadzadeh, M. *An Introduction to the Finite Element Method for Differential Equations*. Wiley, 2021.

[2] Folland, G. B. *Real Analysis. Modern Techniques and Their Applications. 2nd ed*. Wiley-Interscience, 1999.

[3] Johnson, C. *Numerical solution of partial differential equations by the finite element method*. Cambridge university press, 1987.

[4] Mitrea, M., and Monniaux, S. The nonlinear Hodge-Navier-Stokes equations in Lipschitz domains. *Differential Integral Equations 22*, 3-4 (2009), 339–356.

[5] Navier, C. L. Mémoire sur les lois du mouvement des fluides. *Mémoires Acad. Roy. Sci. 6* (1823), 389–440.

[6] Rosén, A. *Geometric Multivector Analysis. From Grassmann to Dirac*. Birkhäuser Advanced Texts: Basler Lehrbücher. [Birkhäuser Advanced Texts: Basel Textbooks]. Birkhäuser/Springer, Cham, [2019], 2019.

[7] Rosén, A. *Partial differential equations from theory to coding*. Unpublished manuscript, 2022.